Soft Matter

PERSPECTIVE

Cite this: DOI: 10.1039/d5sm01239b

Dynamics of particles suspended in field-enhanced microscale flows

Debmalya Halder,[a] Andrew Yee,[b] Minami Yoda*[b] and Shaurya Prakash*[a]

Understanding the dynamics of particles suspended in a flowing liquid is a fundamental fluid mechanics problem. Over the last several decades, significant advances in our theoretical and experimental understanding of these particle-laden flows have been used to manipulate particles in a variety of applications. In particular, recent developments in micro- and nanoscale fabrication and nanotechnology have increased the range of applications, as well as requirements, for manipulating suspended particles with radii less than a few micrometers. We focus here on the surprising and largely unexplained dynamics of neutrally buoyant particles suspended in two common microscale flows, namely Poiseuille and electroosmotic flows, where the particles are subject to both surface forces (*e.g.*, due to pressure gradients) and body forces (*e.g.*, due to electric fields). This perspective review summarizes current developments and identifies opportunities for future advances. Particles suspended in flows can demonstrate both individual and collective behaviors that lead to unusual and unexpected physicochemical hydrodynamics. These dynamics are a long-standing subject of interest, and there has been significant research on the fundamentals of particle–fluid interactions and suspension dynamics because of their relevance to nano- and microscale robotics, drug delivery, biosensing, nanomaterials, optical systems, and biotechnology. The review focuses on the dynamics of nanoscale colloidal particles within confined microscale flows, discussing past discoveries and current state-of-art research, and concluding with suggestions for future research directions.

Received 12th December 2025,
Accepted 18th March 2026

DOI: 10.1039/d5sm01239b

rsc.li/soft-matter-journal

1. Introduction

The behaviour and dynamics of nano- and microparticles suspended in a liquid, with radii ranging from tens of nanometres (nm) to a few micrometres (μm), and their interactions with solid surfaces have been studied in colloid science for over two centuries. The origins of colloidal dynamics can be attributed to Ingenhousz in 1785, who described the "confused" motion of coal dust on the surface of an alcohol layer, an early example of what was later called Brownian motion. Subsequently, the dynamics of particles suspended in a fluid has been a research topic since the early descriptions by Brown (1827),[1] understanding, manipulating, and controlling particles suspended in a fluid remains an active field of research particularly when both the particle and the surrounding surface are charged. In the context of charge-driven interactions, early models of the electrical double layer (EDL), which was assumed to be entirely static, were reported by Helmholtz in 1853[2] and Quincke in 1861.[3] More recently, controlling the dynamics of dilute particle suspensions in flowing, as opposed to quiescent liquids has gained interest due to emerging applications including reconfigurable photonic materials,[4] functional catalytic substrates,[5] tissue engineering,[6] colloidal robotics,[7] and DNA-mediated colloidal crystals.[8] Many of these new applications exploit advanced fabrication methods and material templates, as well as the flow of colloidal particle suspensions in confined microscale geometries to enable precise particle manipulation.[9–11] Consequently, there is growing interest in understanding and controlling the behaviour of flowing particle suspensions in microfluidic environments.[12,13]

Given the breadth of research on these topics and related applications, making substantive advances in this field involves several disciplines.[14] Therefore, this perspective review begins with a brief primer on the history and background while discussing key underlying principles. The review then describes both individual and collective behaviours of nanometer-scale colloidal particles suspended in flowing liquids that lead to unexpected observations suggesting new mechanisms for the observed dynamics. In particular, adding an external force beyond the commonly studied fluid-inertial forces is a new topic of investigation, *i.e.*, "flow+". Among the combinatorial flows with various additional external forces and stimuli (*e.g.*, acoustic, magnetic, thermal), those due to external dc (*vs.* ac)

[a] *Department of Mechanical and Aerospace Engineering, The Ohio State University, Columbus, OH 43210, USA. E-mail: prakash.31@osu.edu*
[b] *Department of Mechanical Engineering, Michigan State University, East Lansing, MI 48824, USA. E-mail: yodamina@msu.edu*

electric fields are perhaps the least studied. Consequently, our understanding of the dynamics of colloidal particles suspended in a flow and subject to electric fields is incomplete compared to other flow+ methods that are used to manipulate suspended nanomaterials. The review closes with a discussion of the current applications, open questions, and author perspectives for future directions.

2. Colloidal assembly mediated by flow+ external stimuli

2.1 Colloids, colloidal assembly, and role of microfluidics

A colloid is a mixture in which one substance, consisting of microscopically dispersed insoluble particles with hydrodynamic diameters of around $O(10^1$ nm) to $O(10^3$ nm), is suspended throughout another substance. In this size range, particles are broadly defined to include macromolecules, micelles, and droplets. While particle dynamics at larger scales are usually dominated by volume (*vs.* surface) forces, the increase in surface area (SA) to volume (V) ratio at these scales means that surface forces play a major role in colloidal particle dynamics. One way to estimate the relative importance of surface (*vs.* volume) forces is to note that $SA/V \propto 1/l_c$ where l_c is the characteristic length scale of the particle. This ratio becomes very large for μm- and nm-sized particles, highlighting the importance of surface forces over body forces at such length scales.[15] Colloids are also subject to phenomena that are negligible at larger scales, such as Brownian motion.[16]

Moreover, inter-particle dynamics may yield structures that have remarkable properties such that the collective particle structures are ''greater than the sum of the parts'', while being distinct from those of the individual constituent particles. These particle structures find applications in drug delivery,[17] biosensing,[18] nanomaterials,[19] optical systems,[20] soft[21] and active materials[22] for colloidal robotics and biotechnology.

The collective particle dynamics, therefore, entail the aggregation of colloidal particles on functional or non-functional substrates, which is a simple way to define the process of colloidal assembly. The suspended particles interact with the substrate, as well as each other. Formally, the definitions for colloidal self-assembly describes a process in which particles organize into ordered structures under the influence of inter-particle interactions. Previously reported strategies for constructing structures from colloidal particles acting as building blocks include evaporation-induced and interface-driven self-assembly, spin-coating techniques, templating with physical moulds, and methods leveraging non-covalent interactions such as hydrophobic effects, hydrogen bonding, electrostatic forces, and π–π stacking.[23] A key limitation of current methods for colloidal self-assembly is their reliance on equilibrium thermodynamics, which makes assembly a relatively slow process which is difficult to scale and therefore, impractical for many engineering applications. Moreover, colloidal self-assembly can also include random aggregation of particles, which may prevent formation of ordered structures.[24]

A significant body of past work has developed and used additional stimuli for directed, more controlled, self-assembly. Furthermore, advances in microfabrication technologies have also made it possible to exploit the breadth of understanding gained over the past two centuries to engineer new particle-assembly structures.[25] Due to the variety of materials and driving forces along with the multi-scale and multi-physics phenomena involved in controlling the colloidal particles in suspension, microfluidics has emerged as a key enabling technology for understanding and realizing colloidal assemblies by providing notable advantages over conventional batch processing systems.[15] The main advantages of using microfluidics include reduced sample and reagent usage, faster processing times, increased sensitivity, lower costs for biological samples, enhanced portability, and potential for continuous and automated operation.[15,26]

Additionally, before going further, it is perhaps important to draw a distinction between two frequently used, apparently interchangeable terms: ''particle assembly''; and ''particle assembly structures'' or ''assembled structures''. ''Particle assembly'' is a general term that refers to the (controlled or uncontrolled) agglomeration of particles on a surface, often governed by thermodynamic rather than kinetic constraints, unless external means are used to enhance control over the aggregation. On the other hand, ''particle assembly structures'' or ''assembled structures'' refer to the kinetics-dominated, controlled accumulation of particles, with or without a template, on a surface to create functional end-pieces. As these particle assemblies are often achieved using external (*e.g.*, electromagnetic, optical) fields, the process is kinetically controlled, as opposed to relying purely on thermodynamic phenomena that may be dominated by diffusion.

Diffusive and kinetic processes in flow-driven assembly occur at different rates due to their distinct scaling. While the diffusion timescale is proportional to the square of particle size or l_c^2, the kinetic timescale for first-order chemical reactions is proportional to the size itself, or l_c. So kinetic processes become faster than diffusive processes for particles at micro- and nanometre lengthscales.[27]

The advantage of adding a flow to the quiescent system can be examined, following the approach reported by Kavokine *et al.*,[28] by comparing the Peclet number (Pe), which characterizes the relative importance of convection and diffusion, and the Reynolds number (Re), which characterizes the relative importance of inertial and viscous forces. As an illustration, using results from recent experiments on assembly of particles suspended in Poiseuille + electroosmotic flow experiments:[29–32] for a particle of radius $a \sim 10^2$ nm as the characteristic length suspended in water with characteristic velocity $\dot{\gamma}a$, Brownian diffusion coefficient $D = 10^{-9}$ m^2 s^{-1}, fluid kinematic viscosity $\nu = 10^{-6}$ m^2 s^{-1}, and characteristic microchannel dimension h of $\sim 10^1$ μm:

$$\frac{\mathrm{Re}}{\mathrm{Pe}} = \frac{\dot{\gamma}a^2/\nu}{\dot{\gamma}ah/D} = \left(\frac{D}{\nu}\right)\left(\frac{a}{h}\right) = O\left(10^{-5}\right) \quad (1)$$

Hence, particle–fluid inertia is negligible. The analysis in eqn (1) also highlights the advantage of particle assembly using

microfluidics where usually viscous effects dominate the fluid mechanics due to relatively small Re.

2.2 Emergence of flow+ methods

The migration of suspended colloidal particles has been an active research topic for decades. As such, colloidal transport and dynamics have been summarized over the last two decades in a number of papers, including reviews of diffusiophoretic migration, *i.e.*, movement due to local chemical gradients of colloids,[33,34] dynamics of active colloids,[35,36] self-assembly of colloidal crystals,[37,38] and colloidal particle transport in porous media.[39,40] Most of these publications are tutorial reviews that summarize previous experimental studies and observations.

The earliest observation of anomalous behaviour of suspended particles in flows, however, dates to reports from the early 1960s of particle migration away from the flow centreline, and hence low flow shear, regions. These observations in laminar pipe flow of dilute suspensions by Segre and Silberberg noted that neutrally buoyant spheres in Poiseuille flow tended to migrate and equilibrate at a radial position approximately 0.6 times the pipe radius from the centre.[41]

Subsequently, the migration force was found to scale with the particle volume, suggesting that this was a body force.[42,43] Saffman theoretically established that the lateral or cross-stream force (*i.e.*, inertial lift) acts on a rigid, neutrally buoyant, purely translating sphere in a viscous flow *via* the slip-shear mechanism.[44] Ho and Leal developed a general theory for inertial lift forces in bounded, pressure-driven flows, accounting for flow curvature[45] and wall effects and calculated the position of lateral equilibrium for translating spheres,[46] which agreed with the previous observations. Asmolov[47] showed that the distance of the equilibrium position from the centreline increases with channel Reynolds number and that there was more than one equilibrium position for higher particle–fluid slip velocities.

Precisely manipulating colloidal particles using inertial lift, which is a body force and hence depends on the particle volume, becomes more challenging when assembling sub-micron particles. External fields, therefore, often provide the additional stimuli to assemble sub-micron particles. These external—namely, acoustic, electric, magnetic, optical and chemical—fields were used not only by themselves, but also in combination with a background shear flow. Fig. 1 shows illustrations of the modulation mechanisms with combinatorial forces.

There are few reviews that provide context and background on the physicochemical hydrodynamics of colloidal particles suspended in a flow, then summarize and link analysis, modelling and experiments.[48–50] There are even fewer reviews of manipulation of suspended polymeric or other dielectric particles in flowing liquids that are also subject to external stimuli—in other words, going beyond convective effects.[51–53] This is surprising given a number of recent studies on migration of particles suspended in Newtonian, and viscoelastic or non-Newtonian, fluids due to (acousto-, magneto-, electro-)phoretic lift,[54,55] and migration driven by externally applied (electric, acoustic, and magnetic) fields.[56–58]

Given the lack of reviews for dielectric particles subject to "flow+" phenomena, the next subsections provide a brief overview of the effects of optical, chemical concentration, magnetic, and acoustic fields combined with fluid flow for manipulation and assembly of colloidal particles. These external fields add modifiable parameters, for example, acoustic frequency and pressure for acoustic fields, magnetic field intensity or particle magnetization for magnetic fields, light polarizability and intensity, for optical fields. These parameters can be varied to create and control acoustic pressure levels, magnetic forces, optical forces, temperature gradients due to absorption, or concentration gradients, all of which can drive diffusiophoresis. All of these methods improve control over particle positioning within the fluid and movement beyond that possible by fluid flow alone, as detailed in a recent review.[51] They have also been discussed symbolically in Fig. 1.

2.2.1 Optophoresis and light-induced self-assembly. Optophoresis refers to the manipulation of colloidal particles using focused light, which acts *via* photo-thermal, photo-chemical, or optical forces to modulate particle activity, interparticle interactions, or local fluid environment. Optophoresis (optical trapping or tweezing) uses focused and relatively high power (O(1 W)) laser light to change the trajectory of the particles with forces of the order 10^2 pN in microchannels *via* electromagnetic gradients and scattering forces, enabling separation based on particle size, shape, refractive index, and polarizability.[59–61] As light is a programmable, non-contact electromagnetic waveform, using light-based forces can also enable reversible and programmable control over colloidal behaviour, enabling precise assembly processes.[62,63] However, this type of manipulation requires an optically transparent fluid.

The capability for light-induced assembly has been demonstrated in various systems, including rotating microgears assembled from hematite-based Janus particles *via* light-induced diffusiophoresis,[64] traveling wave patterns in silver colloids through photo-chemical reactions,[65] UV-triggered reversible clustering of TiO_2–Pt Janus particles,[66] and microfluidic-assisted silica monolayer deposition for light-based gas sensing.[67] Photonic crystals are an emerging technological element for optics and optoelectronics, and colloidal self-assembly provides a bottom-up route for cost-effective and energy-efficient fabrication.[68] These periodic structures, composed of colloids, polymers, or oxides with contrasting refractive indices, have demonstrated broad utility in display technologies,[69] anti-counterfeiting,[70] sensing,[38] photocatalysis,[71] photovoltaics,[72] and structural colour generation.[73]

Despite these advances, optophoresis in most cases requires complex (*e.g.*, precise and stable optical alignment, tuneable power and wavelength) and costly laser systems, associated optics, and is highly sensitive to environmental fluctuations, posing a challenge for widespread adoption. In addition, adoption of optophoresis is limited by its lower structural precision for colloidal assemblies compared with top-down methods. Moreover, there is usually also a need for templating processes, and material limitations, such as size, shape, and refractive index contrast, as well as thermal effects and surface

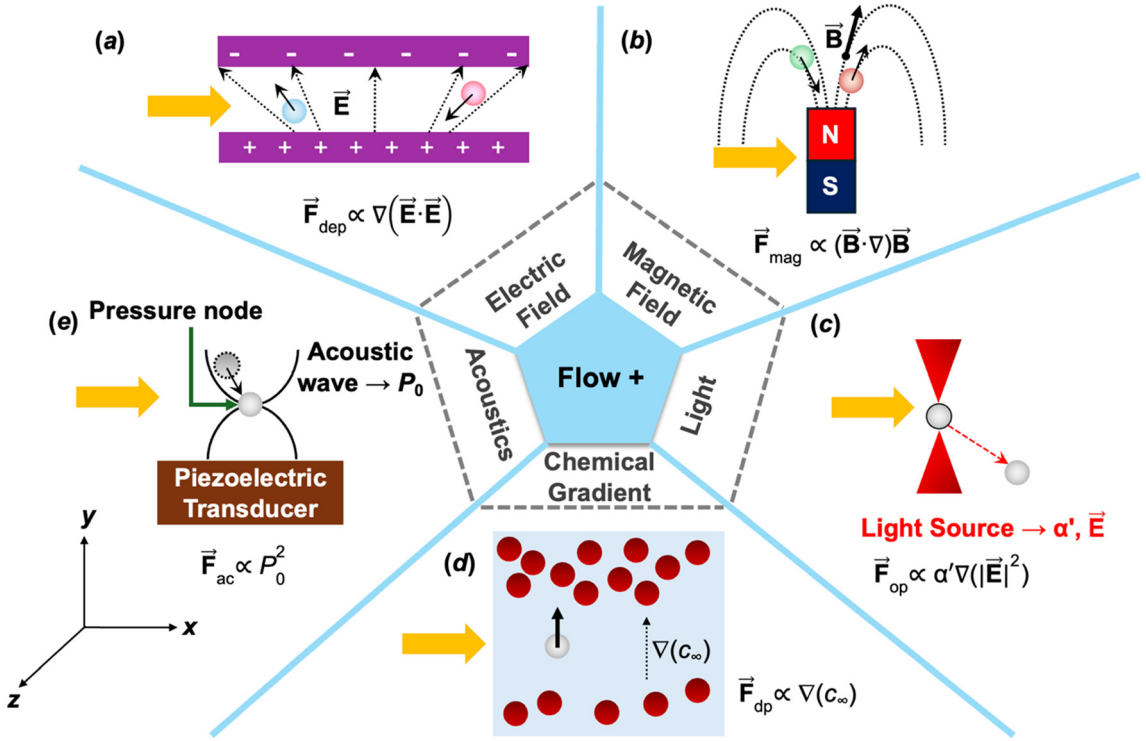

Fig. 1 Illustrations of typical particle manipulation approaches utilizing a combination of flow and external fields. External fields include [clockwise from top left]: (a) electric, (b) magnetic, (c) light, (d) chemical, and (e) acoustic enhancements to the flow. In all cases, a pressure gradient drives flow in the positive x-direction as indicated by the yellow arrow to the right. (a) Dielectrophoresis (DEP) induced by an electric gradient: a particle in a dielectric medium surrounded by a non-uniform electric field $\vec{E}$ (dotted arrows) becomes polarized; the interaction between this polarization and the non-uniform electric field causes particles to migrate either away from (red particle – positive DEP), or towards (blue particle – negative DEP), the direction of the electric gradient. Since the induced force on the particles $\vec{F}_{DEP}$, and thus final cross-stream position, depends on the particle's polarization, the induced field can be used to separate or sort particles based on their polarization. The field, denoted by the dotted arrows, is normal to the y-direction. (b) Magnetophoresis induced by a magnetic gradient $\vec{B}$ (dotted curve with a thick black arrow to indicate direction, so the magnetic field normal to the z-direction): particles with magnetic properties may either move towards (green particle – paramagnetic), or away from (orange particle – diamagnetic), the magnetic north pole due to the induced force on the particles $\vec{F}_{mag}$ (thin black arrows). Particles with different magnetic properties field can be separated or sorted with this method. (c) Optophoresis induced by a light gradient: electromagnetic waves in the form of high-intensity, focused laser light induce polarization in nearby dielectric particles. The light gradient pulls particles to the region of highest light intensity through the induced force $\vec{F}_{op}$. The laser light, often called a light tweezer (red sheet), can be used to manipulate individual particles. So a particle moving in the primary flow direction (positive x-direction) can undergo cross-stream migration (negative y-direction) using light tweezers along the path shown as a red dashed line. The laser light is normal to the x-, or flow, direction. (d) Diffusiophoresis induced by a chemical gradient: a chemical concentration gradient ∇c_∞ (thin black arrow) along the positive y-direction, depicted by regions of varying solute (red circles), causes an induced force $\vec{F}_{dp}$ (thick black arrow) on the particle (grey circle) towards the region of higher solute concentration. (e) Acoustophoresis induced by standing sound waves: transfer of momentum from standing sound waves perpendicular to the x-direction with acoustic pressure P_0 (black curves) to a particle (grey circle) causes particles to migrate from their non-equilibrium (dotted outline) to their equilibrium positions (solid outline) at pressure nodes through induced force $\vec{F}_{ac}$ (black arrow). Particles with different properties settle at different pressure nodes, allowing for separation or sorting.

properties.[68] Nevertheless, optophoresis is a method with a wide range of applications, beyond photonic crystals in optical devices, as also summarized in Borah *et al.*'s 2023 review paper.[68]

2.2.2 Diffusiophoresis. Chemical concentration gradients also enable autonomous self-assembly through particle-generated, *vs.* externally imposed, fields. There are two major types of diffusiophoresis, first is the electrolyte diffusiophoresis which drives particle motion *via* spontaneous electric fields (electrophoresis) and pressure gradients within the Debye layer (chemiphoresis); and second is the non-electrolyte diffusiophoresis, which arises from pressure gradients generated by particle–solute interactions such as steric exclusion or van der Waals forces.[33] Both types of diffusiophoresis have been used to manipulate $a = O(10^1\text{–}10^3\ \mu m)$ particles *via* forces of $O(1\ pN)$ due to electrochemical imbalances.[33] These forces are created by generating controlled solute concentration gradients of $O(10^{-5}\ cm^2\ s^{-1})$ through reactions, evaporation, or localized dissolution, for example.[74] By tuning electrolyte composition, gradient strength, or particle surface charge, directed colloidal transport, focusing, and separation can be achieved without applying external mechanical forces.

Examples of diffusiophoresis include Duan *et al.*, which reported that Ag_3PO_4 particles switched between clustering and dispersal behaviours in response to chemical cues like NH_3 solution or UV light, driven by diffusiophoresis.[63] Wu *et al.* developed a ZnO–SPS ion-exchange system where colloids formed clusters and exhibited directional motion driven by

the pH gradient arising from the production and consumption of H^+ ions.[75] Sridhar *et al.* employed catalytic reactions to create feedback-controlled assembly patterns in chemically active colloidal systems.[76] Bartolo's group described confined ZnO-based colloidal assemblies displayed collective behaviours in response to spatial variations in ion concentrations.[77] Roman and Rembert showed that diffusiophoresis drives colloidal particles towards a piece of calcite affixed in the middle of a microfluidic channel; their aggregation on the surface of this mineral forms a passivation layer that slows dissolution, which could have applications in environmental remediation.[78] Diffusiophoresis is limited, however, because it is:

- a relatively weak effect compared with other colloidal assembly methods,
- short-ranged and short-lived because it relies on transient concentration gradients that often dissipate more rapidly in the presence of flows, and
- complicated by multi-physics and coupled phenomena such as diffusioosmosis.[79]

2.2.3 Magnetophoresis. Magnetic fields can also be used to apply body forces in fluid flows and assemble suspended magnetic colloids *via* dipolar interactions or induced torques with the force scaling as $(\vec{\mathbf{B}}\cdot\nabla)\vec{\mathbf{B}}$, where $\vec{\mathbf{B}}$ is the externally applied magnetic field vector. While the self-assembly of magnetic nanoparticles can be exploited for a variety of applications as highlighted in a review article on self-assembly,[68] a greater degree of control and thereby enhanced applicability is achieved by magnetophoresis, which entails manipulation of colloidal particles by applying a magnetic field gradient that exerts forces on particles with magnetic susceptibility—where the particles themselves are inherently magnetic or embedded in a magnetic medium. Colloids are driven towards, or away from, regions of higher field strength, depending on particle magnetism and that of the surrounding environment, enabling spatial separation based on magnetic contrast.[80]

There are a number of studies that utilize magnetophoresis. Dreyfus *et al.* used rotating magnetic fields to drive colloidal chains that mimicked biological flagella.[81] Yan *et al.* demonstrated that paramagnetic patchy particles could be directed into linear, zigzag, or spiral chains by external magnetic fields.[82] Ray and Fischer engineered colloidal mixtures of paramagnetic and diamagnetic particles in a ferrofluid to form customizable, magnetically ordered phases, transitioning between staggered and uniform bonding patterns by modulating the precession angle and eccentricity of a time-varying magnetic field.[83] Wittman *et al.*[84] developed a novel high-throughput, non-invasive millifluidic platform using magnetophoresis and a pinch-shaped channel design for age-specific fractionation of *S. pastorianus* yeast cells, revealing age-related metabolic shifts through metabolomic and gene expression analyses. More recently, Wu *et al.* used alternating magnetic fields to form aster-shaped clusters of hematite particles.[85] In these studies, magnetic fields of $O(10^{-3}$–10^{-1} T) were used to apply forces in orders of 10^2 pN on $a = O(10^1$–10^3 μm) magnetic materials such as small neodymium iron boron magnets. Magnetophoresis is limited, however, to magnetic particles, and most weakly magnetic particles have almost indistinguishable magnetic susceptibilities, which may limit the efficiency of magnetic particle separations.

2.2.4 Acoustophoresis. Acoustophoresis leverages pressure gradients generated by acoustic waves to manipulate particles. Particles or cells can be manipulated by acoustic radiation forces or pressure nodes by transfer of momentum to particles from the sound waves travelling in the liquid,[86,87] with bulk acoustic waves (BAW)[88] and surface acoustic waves (SAW)[89] being the two common wave types used. Although the forces manipulating these particles arise from pressure gradients due to acoustic stresses acting on the surface of the particle, acoustic waves act on particle volume when the particles are much smaller than the wavelength of sound waves and are hence in the Rayleigh scattering regime.[90,91] Ahmed *et al.* utilized surface acoustic waves to organize colloids into chains and lattices aligned with pressure nodes.[92] Owens *et al.* showed that two-dimensional bulk acoustic standing waves can rapidly and programmably assemble thousands of microscopic particles into size-limited, isotropic and anisotropic architectures—including 3D clusters.[93] Tahamasebipour *et al.* found that introducing geometric asymmetry in micro-acousto-fluidic devices significantly amplifies acoustic forces and improves microparticle trapping efficiency.[94] Recently, Zhong *et al.* introduced an acoustofluidic platform enabling rapid, contactless, frequency-controlled injection and disassembly of microparticles across oil–water interfaces.[95] In these studies, $O(10$–10^3 MHz) frequency acoustic waves were used to manipulate $a = O(10^0$–10^2 μm) particles suspended in a fluid *via* forces as large as 10^2 pN over a piezoelectric solid surface. Acoustophoresis has demonstrated extremely high recovery of target cells at high purities, as great as 99%.[96] However, achieving such high separation efficiencies requires high-frequency signal generators and precisely aligned piezoelectric transducers, making the technique both costly and difficult to implement.

Given some of the drawbacks of using a single field or effect for particle manipulations, there is also a significant body of work that has exploited the addition of flow, or "flow+". Flow-based manipulation of particles with adjuvant forces specifically for separations have led to a new type of flow-based separations called field-flow-fractionation (FFF), usually attributed to Giddings.[97] As the name suggests, FFF has been used to separate particles including cancer cells and extracellular vesicles,[98] micro- and nanoplastics,[99] and plant polysaccharides[100] of different sizes. Broadly speaking, FFF is a subset of flow+ which concerns "fractionation" or segregation of particles in the flow into two groups, in presence of some field, based on previously chosen thresholding criteria.[101,102]

In summary, the broader concept of flow+ encompasses manipulation and arrangement of suspended particles over a range of spatiotemporal scales. Therefore, the term "nonlinear" refers to the dependence of forces on the external fields, or field magnitudes. For example, optical forces of the form $\alpha'\nabla|\vec{\mathbf{E}}|^2$ depend on the gradient of the magnitude of electric field associated with the incident wave squared of where α' is the real component of polarizability.[105] Diffusiophoretic forces

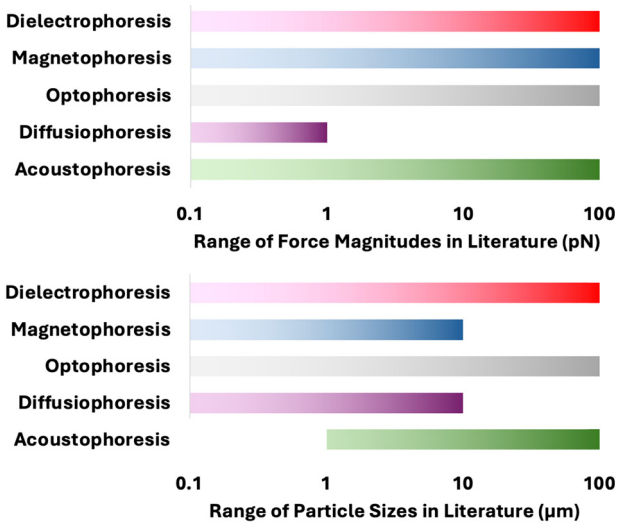

Fig. 2 Order of magnitude comparison. Summary of applied forces over various particle sizes for different particle separation methods using external fields. The figure highlights dielectrophoresis,[104,124,125,155–169] magnetophoresis[64,76–81,99,103,105] optophoresis,[55–61,101] diffusiophoresis,[29,59,70–75,98] and acoustophoresis.[82–90,100,102,104]

are of the form $\nabla(1/\sqrt{c})$ in vicinity of the particle (local force), where c is the electrolyte concentration gradient, although the global force depends on ∇c_∞ where c_∞ is the bulk concentration of the solution.[106] Magnetic forces,[107] on the other hand, are of the form $(\vec{\mathbf{B}}\cdot\nabla)\vec{\mathbf{B}}$, and acoustic forces[108] scale with the square of the acoustic pressure $(P_0)^2$. Fig. 2 lists the commonly reported magnitudes of the various forces[106,108–113] and corresponding sizes of particles used in previous work. Narrowing the focus of this perspectives review, the following sections focus on the manipulations of colloidal particles by electric fields.

3. Fundamentals of electrokinetics: electroosmosis, dielectrophoresis, and electrophoresis

Electrokinetics is defined as the use of electric fields to manipulate flows of electrically responsive fluids. In effect, this approach extends the functionalities outlined in the self-assembly review[68] for charged particles by introducing two additional classes of tuneable parameters—flow and electric field.

3.1 Definitions

Electrophoresis refers to the migration of charged particles under an electric field.[114] Electroosmosis, on the other hand, denotes the movement liquids relative to a charged surface.[115] Dielectrophoresis governs the motion of dielectric particles in non-uniform electric fields, including neutrally charged particles, through field-induced polarization.[116] Electrokinetic phenomena are present in myriad applications in microscale and nanoscale flows due to the impractical scaling of pressure forces to drive flows for reasonable flow rates (pressure scales inversely with fourth power of the characteristic length for the flow) with reducing flow length scales.[15]

Dielectrophoresis (DEP) scales with the gradient of the electric field, and therefore requires a non-uniform electric field.[117] The non-uniformity of the electric field can be used to separate particles of similar physical features such as size even when the particles themselves may be inherently dielectric, since DEP also has a strong (cubic) dependency on size.[118] For colloidal particle manipulations, the dynamics of a spherical particle are usually modelled by coupling quasi-electrostatic fields with transient fluid dynamics of an incompressible Newtonian fluid governed by Maxwell's equations and the unsteady Navier–Stokes equations. The dielectrophoretic force $\vec{\mathbf{F}}_{\mathrm{DEP}}$ on a spherical particle is calculated *via* the Maxwell stress tensor:

$$\vec{\mathbf{F}}_{\mathrm{DEP}} = \oint \left(\overline{\overline{\mathbf{T}}}\cdot\hat{\mathbf{n}}\right)\mathrm{d}A \tag{2}$$

where the Maxwell stress tensor:

$$\overline{\overline{\mathbf{T}}} = \varepsilon\vec{\mathbf{E}}\vec{\mathbf{E}} - \frac{1}{2}\overline{\overline{\boldsymbol{\delta}}}\left(\varepsilon\vec{\mathbf{E}}\cdot\vec{\mathbf{E}}\right) \tag{3}$$

For an equivalent dipole approximation, the force is given by:[119]

$$\vec{\mathbf{F}}_{\mathrm{DEP}} = 2\pi\varepsilon_{\mathrm{f}}a^3\mathrm{Re}\{f_{\mathrm{CM}}\}\nabla(\vec{\mathbf{E}}\cdot\vec{\mathbf{E}}) \tag{4}$$

Here, $\vec{\mathbf{E}}$ is the applied electric field, a is the radius of the spherical particle, $\mathrm{Re}(f_{\mathrm{CM}})$ is the real component of f_{CM}, the Clausius–Mossotti factor:

$$f_{\mathrm{CM}} = \frac{\varepsilon_{\mathrm{p}}^* - \varepsilon_{\mathrm{f}}^*}{\varepsilon_{\mathrm{p}}^* + 2\varepsilon_{\mathrm{f}}^*} \tag{5}$$

where $\varepsilon_{\mathrm{p}}^*$ and $\varepsilon_{\mathrm{f}}^*$ are the complex permittivities of the particle and fluid, respectively. The dielectrophoretic force can therefore be adjusted by tuning the strength of electric field or the radii of the particles (non-linear dependence), and the fluid type and material of the particles, to change the permittivity (fractional linear dependence).

A key feature of electroosmosis, which describes fluid (*vs.* particle) transport, is the electrical double layer (EDL), which presents a model describing the thin layer of counterions formed in the fluid adjacent to a charged interface and includes the diffuse layer arising from diffusion of the counterions into the bulk solution.[52] A common model of this diffuse EDL, the Gouy–Chapman (GC) model,[120,121] couples the Poisson and Boltzmann equations to describe the spatial distribution of charged species in solution and the resultant electric potential field. The GC EDL model defines the Debye screening parameter κ as:

$$\kappa = \sqrt{\left(\frac{2e^2\sum_i z_i^2 c_i^{\mathrm{b}}}{\varepsilon_0\varepsilon_{\mathrm{r}}k_{\mathrm{B}}T}\right)} \tag{6}$$

where z_i and c_i^{b} are the valence and bulk ionic concentration of the ith species in solution, respectively, and k_{B} is the Boltzmann constant. The inverse of the Debye screening parameter is

called the Debye length $\lambda_D \equiv 1/\kappa$. λ_D characterizes the thickness of the EDL and hence the range of electrostatic interactions. So shorter Debye lengths indicate stronger screening and more localized fields. Notably, the Gouy–Chapman model for the diffuse EDL assumes ions as point charges in a continuum solvent while neglecting ion–ion interactions and size effects. The model also assumes Boltzmann distributions for the ion concentrations. Finally, the model is based on single-particle mean-field theory, that is, each ion is treated as if it moves independently in an average (mean) electrostatic potential created by all other charges, rather than explicitly interacting with other ions. The linearization of Poisson–Boltzmann equations using the Debye–Huckel approximations are valuable computationally, but come at the cost of implying small deviations from equilibrium states.[122] Such an approximation may lead to inaccuracies in flow+ configurations where the particle dynamics may deviate significantly from equilibrium conditions. In electrokinetics, the relations between the three primary length scales, namely λ_D, channel diameter and particle size determines the models used to predict the dynamics of particles in confined flows.[123,124] In fact, the EDL plays an important role in determining the lift on particles in the flow,[125–127] which is discussed in the following sections. For a particle of radius, a = 245 nm for the experimental parameters listed in Fig. 2, $a/\lambda_D \sim O(10^1–10^2)$. Thus, the thin Debye layer assumption is valid thereby allowing the extent of the Debye layer to be neglected.

Dielectrophoresis can demonstrate non-linear electrokinetics as shown in eqn (4) due to the dependence on $\nabla(\vec{E}\cdot\vec{E})$. While electrophoresis is often regarded as a linear process, with the force scaling proportionally to the applied electric field,[15] it can also manifest non-linear behaviour.[128] Both experimental[129–131] and numerical[132,133] studies have demonstrated non-linear electrophoresis, wherein the mobility is no longer independent of the field strength, and the electrophoretic velocity scales non-linearly with the electric field.

A recent review[134] highlighted several applications of electrokinetics for colloidal assembly. Some examples of manipulating particle suspensions include positioning and concentrating colloidal quantum dots using a combination of dielectrophoresis (DEP) and ac electroosmosis (ACEO).[135] For example, Juarez *et al.* showed assembly of 2D colloidal crystals through dc electrophoresis and ac dielectrophoresis.[136] In biological systems, electric fields have been used to assemble cellulose-producing bacteria into aligned nanofibril networks[137] and to suppress bacterial adhesion by applying dc-induced electroosmotic flow, generating shear forces that counter surface attachment.[138]

Integrating electrokinetics into microfluidic devices provides additional advantages. Precise low-power electric fields with minimal heating can be applied *via* well-established fabrication techniques. With their high surface-to-volume ratios, microfluidic devices can exploit enhanced surface-driven effects and incorporate multiplexed on-chip multi-stage processes including real-time optical analysis.[139–143] For example, microscale flows coupled with electrokinetics have been used for dynamic single-cell antimicrobial susceptibility testing (AST) incorporating ac dielectrophoresis in high-conductivity buffers,[144] bolus transport and interface shaping in layered viscosities through electrokinetic peristalsis,[145] and label-free DMF–DEP (digital microfluidic dielectrophoresis) for low-voltage droplet handling and high-efficiency yeast cell collection.[146] In most microfluidic applications, the typical dc electrophoretic forces on microparticles in the thin Debye layer limit have magnitudes of $O(10^{-1}–10^1$ pN), while dielectrophoretic force magnitudes can be as large as $O(10^1–10^2$ pN).[147–149]

3.2 Lift forces in shear and/or electroosmotic flows

The concept of inertial lift was introduced in Section 2.2. Earlier models of lift in shearing flows were subsequently expanded to capture the influence of flow parameters such as Reynolds number and slip velocity on particle migration.[47] These models of lift forces driving inertial migration of particles assumed that particle radius, a is much smaller than the critical channel dimension, h, *i.e.*, $a/h \ll 1$. However, as microchannel dimensions decrease or different particle types are used, especially while manipulating colloidal particles with $a/h \sim O(1)$ also arise. To evaluate this assumption, Cherukat,[150] Asmolov,[151] and Su[152] derived correlations relating the inertial lift to non-dimensional flow parameters and particle size. They discovered that lift forces in shear flow have non-linear dependence on a: near the wall, the shear-gradient induced viscous lift depends on particle volume, or a^3, while near the channel centreline, the shear-gradient induced pressure lift depends on a^4. Therefore, the same particle will experience different forces depending on its location within the flow field. Since the origin of the flow-shear lift force is attributed to the slip between the particle and the fluid velocities for colloidal particles and nanomaterials in microscale flows, the role of wall interactions and velocity in determining lift behaviour were also evaluated.[153–155] These studies found that the scaling laws differ from those in classical inertial regime, where dimensionless compliance (how easily a boundary deforms in response to fluid-induced stresses), given as $\mu Va/Gs^2$ (where μ is the dynamic viscosity, V the particle velocity, G the shear modulus of the substrate, and is the particle–wall separation) is much larger at the nanoscale (length scales $<$ 800 nm).[156]

Over the past two decades, a few experimental studies have also observed a repulsive lift force on particles near a wall suspended in uniform EO flow, and hence in the absence of shear,[157] and used this force to separate and manipulate a = 1.5–20 μm particles.[158–160] Modelling studies of this force which is attributed to an electric field gradient arising from the distortion of electric field lines in the relatively narrow gap between the particle and the wall, have found that the force is ''dielectrophoretic-like''—in other words, scales as E^2—in the thin EDL limit where $a/\lambda_D \ll 1$ and E denotes the applied electric field.[161] A recent study considered the case of a ''thicker'' EDL, where surface conduction effects can lead to particle polarization.[162] Interestingly, there remain significant differences between the modelling work and experimental results, though both types of work agree that the lift force is proportional to E^2. The main difference is that the experimental

estimates of the magnitude of dielectrophoretic-like lift force are much (by at least an order of magnitude) greater than the current model predictions.[29,158]

Surprisingly, the effects of simultaneous pressure-gradient driven flow and electric field do not superpose for suspended particle dynamics. The earliest well-documented observations are perhaps those of Alexander and Prieve, who reported shear-induced electrokinetic lift f or particles of radius 8–18 μm suspended in shear flow, attributing the lift to polarization of the particle's EDL in the presence of a wall.[165] Sousa *et al.* renewed interest in using combined pressure-gradient and electric field-driven flows for particle manipulation.[166] Models of shear-induced electrokinetic lift, which is always repulsive, *i.e.*, drives particles away from the charged wall, have considered both Maxwell stress and hydrodynamic effects, and concluded that the force is proportional to the electric field magnitude E.

3.3 Flow+: lift forces in combined Poiseuille and electroosmotic flows

Over a decade ago, Cevheri & Yoda discovered a new electrophoretic lift force in combined Poiseuille and electroosmotic (EO) flows at Re = $O(0.1–1)$ within microchannels containing sub-micron polystyrene (PS) particles.[163] The experimental parameters from their work are tabulated in Table 1 and present an overview of experimental conditions compared to most other published work of the time. For the co-flow configuration, the particles migrated to the centre of the microchannel. Past theoretical work successfully predicted the direction of the lift force causing the particle migration, but the experimentally estimated force and the theoretically predicted force magnitude differed by nearly three orders of magnitude. The discrepancy in lift force magnitudes in the co-flow configuration (pressure gradient and electric field in the same direction) may be attributed to the fact that the flows may not be weakly inertial, as assumed by the current models.[167] Additionally, the analysis of Saffman length l_s (distance between particle centre and point where inertial forces balance viscous forces) by Lochab and Prakash[32] shows that:

$$l_s \sim a/\sqrt{\mathrm{Re_p}} \sim H/\sqrt{\mathrm{Re_c}} \quad (7)$$

where $\mathrm{Re_p}$ and $\mathrm{Re_c}$ are the particle and channel Reynolds numbers, respectively, and H is the characteristic height of the channel. For the range of channel Reynolds numbers considered, $l_s \sim H$ for $\mathrm{Re_c}$ = 1.1 and $l_s \sim 3H$ for $\mathrm{Re_c}$ = 0.1. Moreover, other past theoretical work used regular perturbation analysis.[167,168] When the channel dimensions are comparable to or greater than l_s, the flow around the particle should be split into a domain near the particle (inner flow region) and the far field (outer flow region) to solve the ensuing perturbation problem. Hogg[169] solved such a problem for the migration of non-neutrally buoyant particles in shear flow for $\mathrm{Re_c} \sim 1$. However, no such models exist for combined (shear + electrokinetic) flows with neutrally buoyant particles.

The particles, intended as near-wall flow tracers, exhibited unexpected strong cross-stream migration under counter-flow conditions, *i.e.*, the direction of the applied electric field and pressure gradient were opposite to one another, resulting in the formation of band-like structures. The band formation occurs in three stages: (i) accumulation, where particles are attracted to and concentrate, or ''accumulate'', near the wall of the microchannel; this leads to (ii) band formation, where the particles arrange themselves into a number of unstable ''bands'' that merge and split until they attain a (iii) steady state, when band characteristics, like average fluorescence intensity become fairly consistent or ''stabilized''.[29] Summarizing, band formation starts with particle migration towards, and normal to, the wall. The particles, once concentrated near the wall, interact and form band-like structures. These structures were found to be reversible: in other words, they disassemble when the electric field is turned off.[31] The initial migration depends on the kinematic viscosity of the fluid, and is not observed at higher fluid viscosity.[32]

Perhaps the most surprising observation was that of an attractive force between negatively charged PS particles and the negatively charged silica microchannel wall, with PS particles in dilute suspensions migrating towards the silica walls in weakly inertial flows. The estimated lift forces driving the particles from the microchannel centreline to the walls was ~20 fN, substantially exceeding the additive contributions from EO (~1.6 fN) and Poiseuille (~4.6 fN) flow components.[170] The force scaled approximately as $\dot{\gamma}^{0.4–0.5}$, where $\dot{\gamma}$ indicates the shear rate, and linearly with E, in contrast to previously reported E^2 dependence of dielectrophoretic-like forces in EO flow. Interestingly, the electrophoretic lift force could be either repulsive or attractive depending on the polarity of the applied electric field with respect to the direction of the applied pressure gradient.[12]

These observations suggest analogies between this new electrophoretic lift and the previously discussed inertial lift force, wherein the direction of the force depends on whether the particle leads or lags the local flow. The observed lift also depended on factors such as particle size a, zeta potential ζ, fluid viscosity μ, and electrolyte concentration c_i and the relative magnitudes of shear and electric fields. Khair and Balu (2019) used a perturbation analysis in the limit of small Pe and zero Re (*i.e.*, a quiescent fluid) to find the lift on an uniformly charged, dielectric, rigid sphere.[171] The analysis gave a wall-normal lift force of $O(10^{-5}$ fN), around six orders of magnitude smaller than the experimentally calculated value.[170] The addition of a particle and an external field breaks the symmetry, *i.e.*, reversibility, following the Scallop theorem of Stokes flow.[172]

Table 1 Summary of experimental parameters for observations of cross-stream lift forces in combined Poiseuille and EO co- and counter flow[12,31,163,164]

Particle/flow/fluid property	Value
Radius a [μm]	0.1–0.5
Volume fraction ϕ_∞ [—]	3.3×10^{-5}–3.3×10^{-3}
ζ-potentials [mV]	−77 to −42
Pressure gradient $\Delta p/L$ [Bar m^{-1}]	0.13–1.35
Electric field magnitude E [V cm^{-1}]	20–200
Kinematic viscosity ν [cSt]	0.9–2

In subsequent work by Khair and Kabarowski[167] for weakly inertial flows, the prediction gives the same direction for the force as the experimental observations (*cf.* eqn (8)), but the magnitudes were about three orders of magnitude less than the experimentally calculated values.[32] These underestimates may be due to non-negligible inertial effects in the experiments, with flow Re $\sim$ 0.1–1 for these flows.

In another unexpected observation, counterflow experiments revealed elevated streamwise particle velocities compared to estimates from existing hydrodynamic and electrophoretic models, suggesting the presence of an uncharacterized drag component. It is noteworthy that under steady-state conditions hydrodynamic drag is expected to balance electrophoresis-induced lift.[31,32] The experimental observations suggest that the time scale for the initial stage of near-wall particle accumulation T_0 decreases, suggesting that inertial lift increases, as flow shear rate $\dot{\gamma}$ increases, E increases, ζ_p increases (that is, becomes less negative), a increases, and ϕ_∞ increases.[29] Confocal microscopy studies report that cross-stream particle migration decreases, which suggests that lift also decreases, in co-flow as the fluid kinematic viscosity ν increases, and that the minimum E for band formation increases with electrolyte concentration.[32] Fig. 3 summarizes the progressive developments over the years on these anomalous phenomena.

Furthermore, two modelling advances for weakly inertial flows were reported by Choudhary *et al.*[168] and Khair and Kabarowski.[167] These papers calculated the force on a uniformly charged, spherical particle undergoing electrophoresis in either Poiseuille or shear flow. Specifically, Khair and Kabarowski considered a particle in an unbounded steady simple shear flow. Such a shear flow could approximate flow conditions near a channel wall if wall effects are negligible. Under this flow condition, the lift on a particle of radius a, and defined ζ potential, immersed in a fluid of density ρ, permittivity ε_f, and viscosity μ, and exposed to a streamwise electric field $\vec{\mathbf{E}}$ predicts a force with a magnitude:

$$F_{\text{inertial}}^{\text{lift}} \approx -5.50\frac{\varepsilon_f \zeta a^3 \rho \dot{\gamma} E}{\mu} \tag{8}$$

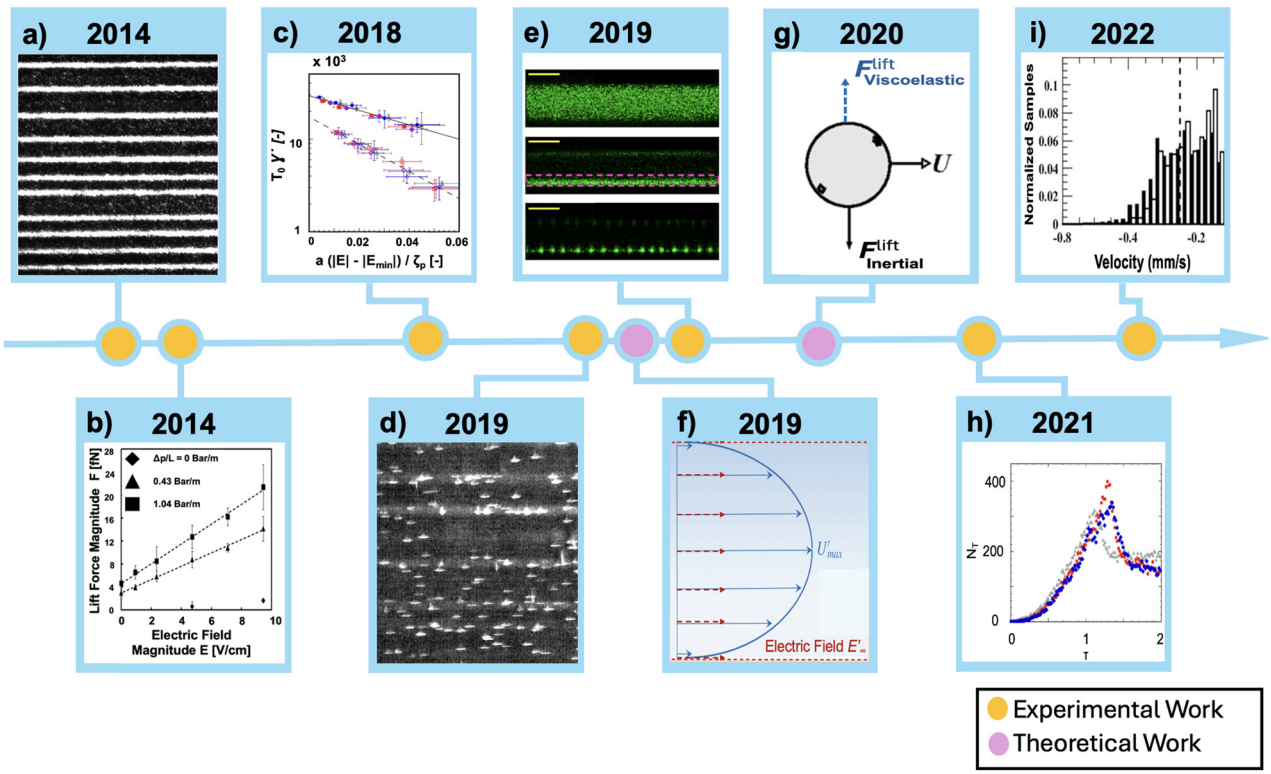

Fig. 3 Observations of particle banding over time. (a) After the discovery of particle banding, research was conducted to determine the fundamental forces governing the phenomenon which was found to occur under many combinations of particle solution and flow conditions.[163,173] (b) The particle migration to the channel wall was governed by a wall-normal lift force which differed in scaling from previous literature. Once near the wall, these particles formed into bands near the channel walls.[12] (c) During the initial stage of band formation, band formation times and spatial frequencies were determined for multiple particle solution and flow parameters process[173] (d) and (e), during this process, the particles in the bulk were found to be depleted.[31,164] (f) and (g) Initial theoretical analytics estimated the magnitude of the lift force.[167,168] (h) Near-wall particle counts during the initial stage of banding showed a $\sim$100 fold increase over band formation.[29] (i) While particles flow generally downstream within the bands, they are hindered due to electrophoresis suppression.[30] Reprinted with permission from: (a) – ref. 163. Copyright 2014, The Royal Society of Chemistry, (b) – ref. 12. Copyright 2014, American Chemical Society, (c) – ref. 173. Copyright 2018, Springer Nature, (d) – ref. 31. Copyright 2019, Springer Nature, (e) – ref. 164. Copyright 2019, Springer Nature, (f) – ref. 168. Copyright 2019, Cambridge University Press, (g) – ref. 167. Copyright 2020, American Physical Society, (h) – ref. 29. Copyright 2021, Wiley-VCH, (i) – ref. 30. Copyright 2022, Wiley-VCH.

The direction of the lift force depends on the direction of $\vec{\mathbf{E}}$, or, alternatively, the particle electrophoretic velocity $\vec{\mathbf{U}}_p$, compared with that of the fluid velocity $\vec{\mathbf{u}}$. If $\vec{\mathbf{U}}_p$ and $\vec{\mathbf{u}}$ are in the same direction (co-flow), the particle is repelled from the wall and migrates towards the channel centre or region of lower shear. In counterflow where $\vec{\mathbf{U}}_p$ and $\vec{\mathbf{u}}$ are in opposite directions, the particle is attracted towards the wall or higher shear region. Therefore, the particle can be attracted to, or repelled from, the wall, consistent with experimental observations.

The density mismatch between a particle and the suspending fluid leads to particle slip in Newtonian shear flows, which in turn causes lateral migration: particles move toward the channel walls when they lead the flow (*i.e.*, their velocity exceeds that of the fluid) and away from the walls when they lag the flow.[169,174] Analogously, in the past work, the electrophoretic number B_e, first suggested by Lochab *et al.*[31] as a new non-dimensional parameter,

$$B_e = (U_p - u)/U_m \quad (9)$$

is negative when the particle lags the fluid, and positive when the particle leads the fluid. In eqn (9) U_p is the electrophoretic particle velocity magnitude, u is the flow speed, and U_m is the (maximum) flow speed at the channel centreline.

While most published work is on Newtonian fluid flows, it is worth mentioning the ''anti-symmetric'' tendencies of particles in non-Newtonian flows, especially as an emerging area for colloidal particle manipulations. Li and Xuan[175,176] and Serhatlioglu *et al.*[177] investigated the dynamics of particles suspended in viscoelastic (*vs.*[177] investigated the dynamics of particles suspended in viscoelastic (*vs.* Newtonian) fluids and observed that particles migrate toward the channel centre-line when they lead the flow (positive electrophoresis) and towards the channel corners/walls when they lag the flow (negative electrophoresis). Li and Xuan[175] showed mode switching (change in elastic property of fluid) from viscoelastic to Newtonian at low polymer concentrations—wherein increasing the PEO concentration causes the migration of leading (or lagging) particles to shift from the centre(or wall)-directed viscoelastic mode to wall-directed (or centre-directed Newtonian mode)—marked by an increased dependency on the electric field strength.

Similar theoretical investigations of these phenomena have been carried out by Li and Xuan,[176] Vishwanathan and Juarez,[178] and Borthakur and Ghosh.[179,180] However, at present there remain significant discrepancies between existing theory and experimental estimates for the extent of particle migration and magnitude of forces driving the particle migration.

4. Current applications of colloidal assembly

Imagine an engineering toolbox that enables printing cellular structures in a gelatinous matrix to develop new bone implants or artificial tissues and organs. Alternately, imagine the ability to create organized structures that bend light to enable faster communication or make objects invisible, or focus and direct heat transfer. These examples are not science fiction: they could all become reality in the next one to two decades based on advances in particle–liquid suspension dynamics, micro- and nanoscale technologies, new materials, and emerging theories and analysis.[7,181–183]

There are a broad variety of methods for manipulating and assembling particles on a surface suitable for different colloidal materials and emerging nanomaterials, including one- and two-dimensional (1D and 2D) materials. One common approach is to guide particles into organized structures using substrate templating[184–189] for directed self-assembly of colloidal particles. The advantages of self-assembly methods include the low external energies required for particle manipulation, and their specificity based on exploiting particle–particle and specific particle-surroundings (*e.g.*, suspending fluid or substrate) interactions. A few of the tremendous range of demonstrated applications and successes of the colloidal science and technology community are highlighted next, followed by a summary of potential areas of future opportunities and critical knowledge gaps.

4.1 Flow-mediated colloidal assembly

Colloidal particles of radii a = 0.05–0.5 μm have been extensively characterized and studied for more than a century in a variety of applications, including as building blocks for engineering structures. The over-arching goal of colloidal assembly is to design and generate functional material assemblies where the ''whole is greater than the sum of the parts''—in other words, the assembly outperforms its constituents, with macroscopic properties distinct from those of the individual constituent particles.[23,190] Such assemblies have myriad applications in both biotic and abiotic systems, such as light and energy harvesting[191,192] and biological detection.[193,194]

As self-assembly processes are inherently subject to thermodynamic equilibrium-dominated kinetics, these assembly methods tend to be slow and limited in both yield and the realizable size of the assembled structures. Therefore, rapid and scalable fabrication of engineered-structures at the mm- or cm-scale from nm-scale building blocks, involving assembly over more than four orders of magnitude in length scale, remain a significant technical challenge. These challenges have inspired innovative new tools and approaches,[13] as also reviewed by Li *et al.*[50,195] and Cai *et al.*[196] Most of the previous examples of colloidal particle assembly using light, sound, magnetic, or electric fields to enhance fluid inertial effects are limited to manipulating micron-scale particles, cells, and other dielectric materials within microchannels[151,197–200] or microfluidic devices within quiescent suspensions—*i.e.*, in the absence of a background flow.

However, it is difficult without background flow to control the dynamics and size of the particle aggregates once formed, or to scale (up) particle aggregation. Moreover, the aggregates assembled in quiescent solutions are rarely ordered structures that can provide the dynamic functionality that would be required for either programmable materials or functional

assembly units. On the other hand, continued development of alternative emerging techniques, such as ''flow+'' methods that allow systematic control over particle migration and the demonstrated capability to create long (mm-scale) but narrow (few particle diameters) particle structures from sub-micron particles could enable a new-class of particle assemblies yielding structures that act as ''functional legos''. We envision functional legos to form a new class of ordered structures built from colloidal particles with assembly length scales extending to millimetres to even centimetres. Additionally, these structures are envisioned to be assembled from 1D-to-3D structures with heterogeneous integration of materials.

Interestingly, we note, after reviewing the large body of available literature available, there is far less discussion of flow-mediated assembly of colloidal particles. Most of the past work on flow-mediated assembly has focused on 1D structures a single particle in width, referred to as strings, chains, or bands.[201] For example, a number of groups have studied the formation of 1D structures aligned with the streamwise direction in high-shear ($\dot{\gamma} \sim O(10^1\ s^{-1})$) flows of dilute colloidal suspensions.[202–204] Interestingly, the approach to flow+ developed by our team has the potential for high-throughput fabrication of 1D and 2D structures[13] with initial demonstrations of heterogeneous assembly.[31] More broadly, flow-mediated methods have been successfully employed for a variety of applications involving both living and non-living systems.

On the other hand, laser illumination of an otherwise quiescent suspension has been used in optofluidics to generate local flows that convect particles away from fouled surfaces.[205] Light-driven diffusio-osmosis has been used to assemble suspended porous colloidal silica microspheres ($a \approx 2.5$ μm with ~6 nm pores) with photosensitive surfactants (''photo-soap'') on a solid glass surface and organize the particles into patterns using a spatially modulated light source.[206] A similar approach has been used to manipulate active biological materials, such as *Pseudomonas putida*.[207]

A recent review[208] discussed using bulk acoustic waves—those propagating normal to the surface of the material generating the acoustic wave, and surface acoustic waves (SAW) propagating parallel to the surface of interest—to manipulate colloidal particles. Piezoelectric materials are often used in microfluidics to generate acoustic waves in the fluid medium, and such acoustic-wave colloidal manipulations have been used in materials assembly and synthesis,[209–212] microreactors,[213] and cell sorting.[214–216]

As noted previously in this perspective, one often-overlooked flow+ method uses electric fields as external stimuli, particularly in a flowing particle suspension. One of the earlier demonstrations of particle aggregation was attributed to flow-induced by distortions in the electric field due to inhomogeneities in the EDL on the electrode surfaces caused by colloidal particles on these electrodes.[217] In these early experiments, a = 0.5–1 μm PS beads suspended in an aqueous sodium azide solution were placed in a 50 μm gap between oxide-capped silicon and indium tin oxide surfaces. Both dc and ac electric fields applied across the gap led to particle aggregates with possible hexatic states in the assembled structures.[217] The electric field in the combined flow may be exploited to influence particle movements. Inhomogeneities in the applied electric field and/or or surface charge are known to generate micro-vortices or locally reversed flows in microchannels and near electrode interfaces.[218–220] Such flows with local micro-vortices due to engineered surface charge or electric field discontinuities have been used to manipulate colloidal particles as well as microbeads,[221–223] 2D materials,[224] and biomolecules such as proteins.[225]

4.2 Limitations in colloidal assembly, converging research pathways and emerging directions

As defined in Section 2.2.4, flow+ mobilizes external fields for deposition of particles with similar physical or chemical properties on a substrate. One of the critical challenges in assembly of colloidal materials, therefore, lies in heterogeneous assembly where materials with distinct properties can be integrated to a mm- or cm-scale structure. For example, in the context of building large scale photonic crystals, materials with distinct optical properties need to be integrated into an organized structure with assembly defects that are at or below the wavelength of the light that interrogates the crystals. Given the physical scale for such devices, non-equilibrium assembly methods that will enable successful scalable fabrication of fully programmable colloidal architectures are required.

A potential solution may arise from an emerging field that has very recently been exploited for templating colloidal superstructures: using nucleic acids; specifically, deoxyribonucleic acid (DNA), for DNA-assisted self-assembly.[231,232] At the nanoscale, it is now feasible to generate colloidal crystals with advanced metamaterial properties such as tuneable structure, size or morphology,[22,233] as well as functional nanodevices like micromirrors and 3D arrays of Josephson junctions.[234,235] At the microscale these mixed assembles of colloidal particles with DNA assemblies exhibit optical metamaterial characteristics like structural coloration in the visible range and complete photonic bandgaps in the near-infrared spectrum.[229,230] These technology demonstrations suggest possibilities in the near- to medium term to develop programmable nanophotonic devices that can enable configurable optical properties and functionality.[62]

In the longer term, building on the progress made in colloidal crystal engineering with DNA[236] and the spatial organization that can be realized using nucleic acid frameworks[237] could lead to ''nucleic acid-colloid frameworks'' where DNA-functionalized particles of various materials and functionalities are integrated into a nucleic acid lattice. With appropriate design and optimization, these frameworks could provide a scalable high-yield pathway to 3D heterogeneous assembled structures that overcome the entropic limitations of self-assembly.

Extending nucleic acid assembly, another emerging technology is in RNA-mediated self-assembly, which offers distinct advantages over DNA-based approaches by acting not only as a structural scaffold but also as a chemically active template, enabling dynamic and multifunctional assembly processes, with increased specificity. For instance, RNA has been used to

direct the nucleation and growth of CdS nanoparticles into tuneable nanostructures with enhanced and size-dependent optical properties, facilitating bottom-up fabrication of optoelectronic materials.[238] In another approach, enzymatic cycles of RNA synthesis and degradation were coupled to colloidal aggregation, enabling autonomous and reversible assembly behaviour controlled by local biochemical energy inputs and spatiotemporal gradients.[239] Additionally, RNA has served as a scaffold for ''nanojacketed'' hybrid nanobiocomposites, where Ag nanoparticles stabilized on POMA fibrils enhanced electrical conductivity and enabled diode-like functionality through p–n-type interfacial interactions.[240]

Showcasing the breadth of colloidal assembly applications, these assemblies have also benefited regenerative medicine by generating both scaffold-based and scaffold-free structured templates for guiding tissue regeneration in injured or atrophic regions.[241,242] These assemblies can mimic the extracellular matrix by arranging biocompatible colloidal particles, including cell-laden microgels or hydrogel-coated nanoparticles, into hierarchical frameworks with tailored mechanical and biochemical properties to help regenerate damaged tissues, for example, in wound healing.[243,244] Colloids have also been used in fluid resuscitation,[245] drug delivery[246] and wound healing.[156]

As demonstrated throughout this article, colloids span multiple spatial scales—for instance clouds, where microscopic water droplets or ice crystals are dispersed in air. These droplets, though individually on the order of micrometres, collectively form large, visible cloud structures that extend across meters, even kilometres.[247] Therefore, what starts off at the nano- and micrometre length scales can ultimately manifest at macroscopic scales of metres, thus spanning nearly seven orders of magnitude! Even for artificial structures like photonic crystals, nanoscale building blocks can organize into highly ordered lattices extending over tens of micrometres to several millimetres.[248] Within these systems, the functional length scale emerges from the coupling between nanoscale particle arrangement and macroscale optical behaviour, where the periodic spacing—comparable to the wavelength of visible light—produces iridescent colours through

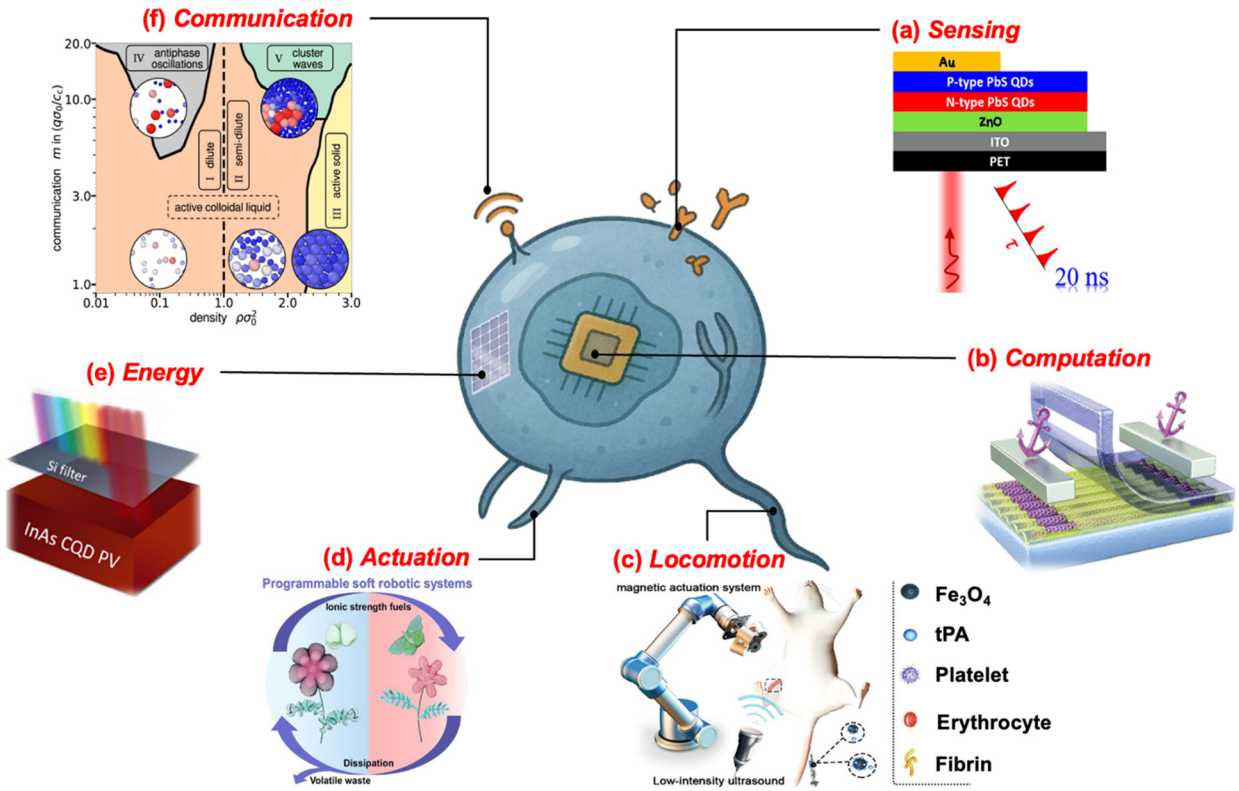

Fig. 4 Schematic suggesting use of multiple technologies towards next-generation colloidal assemblies: (a) sensing: an ultra-flexible colloidal quantum dot (QD) photodetector that demonstrated rapid response and efficient carrier extraction[226] (reprinted with permission from ref. 226. Copyright 2025, American Chemical Society); (b) computation: a novel self-anchoring process, which uses a yttrium oxide sacrificial layer and source–drain electrode anchoring, effectively suppressing carbon nanotube (CNT) stacking during fabrication of aligned CNT field-effect transistors[227] (reprinted with permission from ref. 227. Copyright 2025, American Chemical Society); (c) locomotion: cilia-mimic locomotion of magnetic colloidal particles using magnetic field and ultrasound facilitates better infiltration of thrombolytic drugs and enhances imaging quality[85] (reprinted with permission from ref. 85. Copyright 2025, Wiley-VCH); (d) actuation: ionic fuel-powered soft robotics constructed by programmable salt-responsive actuators exhibit tunable bending orientations, amplitudes, and durations, with consistent cyclic actuation enabled by fuel replenishment[228] (reprinted with permission from ref. 228. Copyright 2025, Elsevier); (e) energy harvesting: lead-free indium-arsenide QD infrared photovoltaics used for harvesting solar energy[229] (reprinted with permission from ref. 229. Copyright 2025, Wiley-VCH); (f) communication: two-dimensional Brownian dynamics simulations of catalytically active, non-motile hydrogel colloids revealed a wide range of nonequilibrium structures and active phases[230] (reprinted with permission from ref. 230. Copyright 2025, Nature Portfolio).

Bragg diffraction.[249] Therefore, starting at the nm scale gives access to a much wider range of actuation, harnessing physics across a broad range of length scales.

Colloidal megastructures of the future can be expected to harvest, exploit and selectively radiate energy within a single integrated unit, thereby enabling energy conservation while simultaneously providing directional heating and lighting. Developments in this direction may be enabled by plasmonic nanoparticles—metallic nanoparticles that exhibit unique optical properties due to the collective oscillation of their free electrons when interacting with light.[250–252] Plasmonic nanoparticle assemblies have already shown enhanced light absorption and heat generation.[253] Similarly, self-assembled films have shown promise for heterogeneous catalysis,[254] electrochemical sensing,[255] and anti-reflective coatings for improved photovoltaic efficiency. Magnetic nanoparticle chains have even been used as nano-stirrers inside microdroplets, overcoming mass transfer limitations at the microscale.[256] However, realizing larger structures for smart windows to heat or cool buildings, for example, requires overcoming another challenge in heterogeneous assembly: the lack of intermediate-scale methods to manipulate the surface chemistry of colloidal nanostructures (*vs.* the bulk chemistry of the constituent particles) without adversely affecting either the assembly methods or the engineered properties of the final larger structure.

Thus far we highlight applications based on assembly of inanimate particles using field forces; however, a futuristic implementation—a "smart"-er extension of active colloids[257]—are colloidal robots (CRs), envisaged as swarms of mobile units each having length scales of the order of colloidal particles. CRs have been proposed as another emerging domain for multifunctional micro-machines, bridging the realms of materials science, robotics, and nanotechnology with capabilities spanning logic, sensing, actuation, energy harvesting, and autonomous control.[7] Fig. 4 depicts how research advancing in distinct domains, often making parallel progress, could be leveraged to mitigate the of the challenges in colloidal robotics. As scientific demonstrations and technological advances continue, one of the main impediments is the lack of a physicochemically-based and multi-physics theory describing kinematics and dynamics of the assembly processes, including emerging topics such as colloidal robotics. Much of the current theoretical understanding of colloidal dynamics relies on applying single-particle force models to systems that, in reality, involve dense particle swarms where inter-particle hydrodynamic, electrostatic, and possibly collective effects are probably non-negligible. This discrepancy may partially explain why experimentally measured lift forces are often found to be 3–4 orders of magnitude greater than theoretical predictions.[29] Therefore, if the motion of these particles to yield functional structures can be precisely predicted and controlled—or ideally rendered autonomous—they hold significant potential for orchestrating the formation of complex mesoscale architectures from colloidal building blocks and thereby realize the potential of modular building blocks—functional legos.

Current "state of the art" approaches for colloidal assembly, whether driven by light, electrical, magnetic and acoustic fields, or chemical gradients, are founded, for the most part, on serendipitous *ad hoc* observations.[62,258–261] They are also limited in terms of the particle materials that can be assembled despite subsequent development—to photochemically or chemically active,[64,262] magnetically susceptible,[263] or dielectric particles,[264] for example. Improved fundamental physics- and chemistry-based theories and models, especially those that focus on more "materials-agnostic" assembly approaches (based, for example, on differential particle–fluid inertia[265] and acoustic fields[266]) could provide the understanding required to optimize assembled structures, functionalities, and yield for a broader range of materials.

5. Summary and future outlook

Colloids—suspensions of nano- and microscale particles in liquids—are not only ubiquitous in nature,[267] but can also be harnessed to engineer functional structures from the bottom up. The engineered structures, so-called colloidal assemblies, span multiple length scales, from the nanometre range (Debye length, chemical,[268] and magnetic[269] interactions), to the submicron regime (wavelength of light and thereby electromagnetics[270]), and further to the sub-millimetre and centimetre scales governed by acoustic wavelengths,[271] making colloids inherently multiscale and multi-physics. Just as living and non-living entities may be constructed out of colloidal units, the functional surfaces used to mediate colloidal particle aggregation may be abiotic or biotic and spanning broad length scales, as evident in the discussions of depositions of colloidal particles on surfaces as simple as glass or PDMS, the surface of the mineral, or something elusive as DNA and even RNA facilitated colloidal assembly. Furthermore, the inherent strength of colloidal assembly lies in the fact that it can be tapped in various ways to create not just homogeneous but also heterogeneous assemblies of particles—be it different characteristics of same material particles, or assemblies of different materials, much like functional legos—by leveraging the use of flows and external fields to introduce additional control variables, giving rise to the emerging domain of flow+.

Throughout this perspectives review, we have identified challenges and opportunities for continued advances in colloidal assembly, primarily placing the existing knowledge within the context of flow+ approaches for particle manipulation. Starting with a brief history and subsequent development of this field, as well as the current state-of-art for particle manipulation, with applications in separation, focusing, trapping, assembly, and sensing of particles and their responses in microfluidics. Several critical knowledge gaps have been identified, including (i) the need for physicochemically-based and multi-physics theoretical and computational model development; (ii) possibilities for discovering and exploiting novel microscale flow phenomena; and (iii) the need for improved integration of models with experimental data and observations.

Among the various challenges, fundamental understanding of the experimental observations is limited by significant gaps in theoretical models. One of the potential reasons for the lack of appropriate theoretical models arises due to the complexity and difficulty in modelling the nonlinear coupling between hydrodynamic interactions, electrokinetic slip, and inertial effects—all for multi-particle suspensions. It is highly likely that addressing the multi-physics scale of this problem requires integration of a suite of techniques including kinetic theory, nonlinear stability analysis, asymptotic and matched expansions, phase-field models, and bifurcation theory to capture multiscale interactions. It is also likely that as experimental data sets and observations continue to grow, artificial intelligence-based modelling may be required.

The key goal of colloidal particle manipulation research is therefore to design, then build (assemble) functional materials with colloids as building blocks so that the properties of the aggregate structures or assemblies are distinct from individual colloidal particles. The admittedly limited set of flow+ particle manipulation approaches reviewed here are, with minimal modification, relevant to functional building blocks for sensing, locomotion and energy management, and could, with further development, be used to assemble building blocks for computation and communication functions. By assembling $O(0.01–1\ \mu m)$ particles into engineered microstructures, such functional legos would bridge the technology gap between bottom-up assembly methods and top-down manufacturing methods—and continue the rich legacy of advances in colloidal particle dynamics and assembly.

Author contributions

D. H. – investigation, writing – original draft, writing – review & editing; A. Y. – writing – original draft, writing – review & editing; M. Y. – conceptualization, supervision, writing – review & editing; S. P. – conceptualization, funding acquisition, supervision, writing – review & editing.

Conflicts of interest

There are no conflicts to declare.

Data availability

No primary research results, software or code have been included and no new data were generated or analysed as part of this review.

Acknowledgements

The U.S. Department of Defense supported this work through the Peer-Reviewed Cancer Research Program under Grant CA210874 and supported by the Mechanical Sciences Division of the U.S. Army Research Office (contract W911NF-16-1-0278 and W911-NF-1-0144).

Notes and references

1 R. Brown, *Philos. Mag.*, 1828, **4**, 161–173.
2 H. Helmholtz, *Ann. Phys.*, 2006, **165**, 211–233.
3 G. v Quincke, *Ann. Phys.*, 1861, **189**, 513–598.
4 J. Chen, X. Li, Q. Liang, B. Zeng, J. Zheng, C. Wu, Y. Cao, J. Yang and J. Tang, *Matter*, 2024, **7**, 3554–3566.
5 A. M. Brooks, M. Tasinkevych, S. Sabrina, D. Velegol, A. Sen and K. J. M. Bishop, *Nat. Commun.*, 2019, **10**, 495.
6 A. Khademhosseini, R. Langer, J. Borenstein and J. P. Vacanti, *Proc. Natl. Acad. Sci. U. S. A.*, 2006, **103**, 2480–2487.
7 A. T. Liu, M. Hempel, J. F. Yang, A. M. Brooks, A. Pervan, V. B. Koman, G. Zhang, D. Kozawa, S. Yang, D. I. Goldman, M. Z. Miskin, A. W. Richa, D. Randall, T. D. Murphey, T. Palacios and M. S. Strano, *Nat. Mater.*, 2023, **22**, 1453–1462.
8 Z. Li, Y. Lim, I. Tanriover, W. Zhou, Y. Li, Y. Zhang, K. Aydin, S. C. Glotzer and C. A. Mirkin, *Sci. Adv.*, 2024, **10**, eadp3756.
9 L. A. Holland and L. D. Casto-Boggess, *Annu. Rev. Anal. Chem.*, 2023, **16**, 161–179.
10 S. Shen, X. Qin, H. Feng, S. Xie, Z. Yi, M. Jin, G. Zhou, E. M. Akinoglu, P. Mulvaney and L. Shui, *Adv. Sci.*, 2022, **9**, 2203341.
11 L. Wang and J. Wang, *Nanoscale*, 2019, **11**, 16708–16722.
12 N. Cevheri and M. Yoda, *Langmuir*, 2014, **30**, 13771–13780.
13 V. Lochab, E. D. Ewim and S. Prakash, *Soft Matter*, 2023, **19**, 2564–2569.
14 V. N. Manoharan, *Science*, 2015, **349**, 1253751.
15 S. Prakash and J. Yeom, *Nanofluidics and Microfluidics: Systems and Applications*, William Andrew, 2014.
16 K. Zhao and T. G. Mason, *Rep. Prog. Phys.*, 2018, **81**, 126601.
17 M. Beija, R. Salvayre, N. Lauth-de Viguerie and J. D. Marty, *Trends Biotechnol.*, 2012, **30**, 485–496.
18 P. D. Howes, R. Chandrawati and M. M. Stevens, *Science*, 2014, **346**, 1247390.
19 W. Baek, H. Chang, M. S. Bootharaju, J. H. Kim, S. Park and T. Hyeon, *JACS Au*, 2021, **1**, 1849–1859.
20 Y. Zhang, D. D. Xu, I. Tanriover, W. Zhou, Y. Li, R. López-Arteaga, K. Aydin and C. A. Mirkin, *Nat. Photonics*, 2024, **19**, 20–27.
21 K. Ueno, *Polym. J.*, 2018, **50**, 951–958.
22 K. J. M. Bishop, S. L. Biswal and B. Bharti, *Annu. Rev. Chem. Biomol. Eng.*, 2023, **14**, 1–30.
23 Z. Xu, L. Wang, F. Fang, Y. Fu and Z. Yin, *Curr. Nanosci.*, 2016, **12**, 725–746.
24 X. Xia, H. Hu, M. P. Ciamarra and R. Ni, *Sci. Adv.*, 2020, **6**, eaaz6921.
25 C. Zeng, M. W. Faaborg, A. Sherif, M. J. Falk, R. Hajian, M. Xiao, K. Hartig, Y. Bar-Sinai, M. P. Brenner and V. N. Manoharan, *Nature*, 2022, **611**, 68–73.
26 A. T. Conlisk, *Essentials of Micro- and Nanofluidics: With Applications to the Biological and Chemical Sciences*, Cambridge University Press, 2012.
27 E. W. Thiele, *Ind. Eng. Chem.*, 1939, **31**, 916–920.
28 N. Kavokine, R. R. Netz and L. Bocquet, *Annu. Rev. Fluid Mech.*, 2021, **53**, 377–410.

29 A. J. Yee and M. Yoda, *Electrophoresis*, 2021, **42**, 2215–2222.
30 A. J. Yee and M. Yoda, *Electrophoresis*, 2022, **43**, 2093–2103.
31 V. Lochab, A. Yee, M. Yoda, A. T. Conlisk and S. Prakash, *Microfluid. Nanofluid.*, 2019, **23**, 134.
32 V. Lochab and S. Prakash, *Soft Matter*, 2021, **17**, 611–620.
33 D. Velegol, A. Garg, R. Guha, A. Kar and M. Kumar, *Soft Matter*, 2016, **12**, 4686–4703.
34 J. T. Ault and S. Shin, *Annu. Rev. Fluid Mech.*, 2025, **57**, 227–255.
35 J. L. Moran and J. D. Posner, *Annu. Rev. Fluid Mech.*, 2017, **49**, 511–540.
36 A. Zöttl and H. Stark, *Annu. Rev. Condens. Matter Phys.*, 2023, **14**, 109–127.
37 J. Hou, M. Li and Y. Song, *Angew. Chem., Int. Ed.*, 2018, **57**, 2544–2553.
38 Y. Hu, Z. Tian, D. Ma, C. Qi, D. Yang and S. Huang, *Adv. Colloid Interface Sci.*, 2024, **324**, 103089.
39 B. Huang, Z. Yuan, D. Li, M. Zheng, X. Nie and Y. Liao, *Environ. Sci.: Processes Impacts*, 2020, **22**, 1596–1615.
40 D. Deb and S. Chakma, *Int. J. Environ. Sci. Technol.*, 2022, **20**, 6955–6988.
41 G. Segre and A. Silberberg, *Nature*, 1961, **189**, 209–210.
42 G. Segré and A. Silberberg, *J. Fluid Mech.*, 1962, **14**, 115–135.
43 G. Segré and A. Silberberg, *J. Fluid Mech.*, 1962, **14**, 136–157.
44 P. G. Saffman, *J. Fluid Mech.*, 1965, **22**, 385–400.
45 B. Ho and L. Leal, *J. Fluid Mech.*, 1974, **65**, 365–400.
46 B. Ho and L. Leal, *J. Fluid Mech.*, 1976, **76**, 783–799.
47 E. S. Asmolov, *J. Fluid Mech.*, 1999, **381**, 63–87.
48 N. Vogel, M. Retsch, C.-A. Fustin, A. Del Campo and U. Jonas, *Chem. Rev.*, 2015, **115**, 6265–6311.
49 S. Zhang, Y. Wang, P. Onck and J. den Toonder, *Microfluid. Nanofluid.*, 2020, **24**, 24.
50 Z. Li, Q. Fan and Y. Yin, *Chem. Rev.*, 2022, **122**, 4976–5067.
51 H. Cha, H. Fallahi, Y. Dai, D. Yuan, H. An, N. T. Nguyen and J. Zhang, *Lab Chip*, 2022, **22**, 423–444.
52 A. Alizadeh, W. L. Hsu, M. Wang and H. Daiguji, *Electrophoresis*, 2021, **42**, 834–868.
53 D. Yuan, Q. Zhao, S. Yan, S.-Y. Tang, G. Alici, J. Zhang and W. Li, *Lab Chip*, 2018, **18**, 551–567.
54 J. Zhou and I. Papautsky, *Microsyst. Nanoeng.*, 2020, **6**, 113.
55 T. Zhang, D. Di Carlo, C. T. Lim, T. Zhou, G. Tian, T. Tang, A. Q. Shen, W. Li, M. Li, Y. Yang, K. Goda, R. Yan, C. Lei, Y. Hosokawa and Y. Yalikun, *Biotechnol. Adv.*, 2024, **71**, 108317.
56 S. Shin, *Biomicrofluidics*, 2023, **17**, 031301.
57 F. Hossein and P. Angeli, *Biophys. Rev.*, 2023, **15**, 2005–2025.
58 J. Philip, *Adv. Colloid Interface Sci.*, 2023, **311**, 102810.
59 A. Ashkin, *Phys. Rev. Lett.*, 1970, **24**, 156–159.
60 A. Atajanov, A. Zhbanov and S. Yang, *Micro Nano Syst. Lett.*, 2018, **6**, 2.
61 P. Paiè, T. Zandrini, R. M. Vázquez, R. Osellame and F. Bragheri, *Micromachines*, 2018, **9**, 200.
62 Y. Huang, C. Wu, J. Chen and J. Tang, *Angew. Chem., Int. Ed.*, 2024, **63**, e202313885.
63 W. Duan, R. Liu and A. Sen, *J. Am. Chem. Soc.*, 2013, **135**, 1280–1283.
64 J. Palacci, S. Sacanna, S.-H. Kim, G.-R. Yi, D. J. Pine and P. M. Chaikin, *Philos. Trans. R. Soc., A*, 2014, **372**, 20130372.
65 H. Chen, Y. Wang, Y. Liu, Q. Zou and J. Yu, *ACS Nano*, 2022, **16**, 16281–16291.
66 S. Che, J. Zhang, F. Mou, X. Guo, J. E. Kauffman, A. Sen and J. Guan, *Research*, 2022, **2022**, 9816562.
67 V. Zaytsev, A. Kuzin, K. Panda, V. Chernyshev, I. Florya, F. S. Fedorov, V. Kovalyuk, A. Golikov, P. P. An, B. N. Khlebstov, M. Chetyrkina, A. G. Nasibulin, G. Goltsman and D. A. Gorin, *Nanoscale*, 2024, **16**, 17365–17370.
68 R. Borah, K. R. Ag, A. C. Minja and S. W. Verbruggen, *Small Methods*, 2023, **7**, e2201536.
69 W. Liu, G. Li, C. Chen, J. Liu and Z.-Y. Li, *J. Mater. Chem. C*, 2024, **12**, 6588–6595.
70 Y. Gao, K. Ge, Z. Zhang, Z. Li, S. Hu, H. Ji, M. Li and H. Feng, *Adv. Sci.*, 2024, **11**, e2305876.
71 H. Li, C. Cheng, Z. Yang and J. Wei, *Nat. Commun.*, 2022, **13**, 6466.
72 C. Yuan, Y. Yang, L. Huang and Y. Xiao, *ACS Omega*, 2024, **9**, 9720–9727.
73 H. Chen, J. Wei, F. Pan, T. Yuan, Y. Fang and Q. Wang, *Adv. Mater. Technol.*, 2025, **10**, 2400865.
74 J. L. Anderson and D. C. Prieve, *Sep. Purif. Methods*, 1984, **13**, 67–103.
75 C. Wu, J. Dai, X. Li, L. Gao, J. Wang, J. Liu, J. Zheng, X. Zhan, J. Chen and X. Cheng, *Nat. Nanotechnol.*, 2021, **16**, 288–295.
76 V. Sridhar, F. Podjaski, J. Kroger, A. Jimenez-Solano, B. W. Park, B. V. Lotsch and M. Sitti, *Proc. Natl. Acad. Sci. U. S. A.*, 2020, **117**, 24748–24756.
77 A. Bricard, J. B. Caussin, N. Desreumaux, O. Dauchot and D. Bartolo, *Nature*, 2013, **503**, 95–98.
78 S. Roman and F. Rembert, *Phys. Rev. Fluids*, 2025, **10**, L032501.
79 R. E. Migacz and J. T. Ault, *Phys. Rev. Fluids*, 2022, **7**, 034202.
80 M. Benelmekki, L. M. Martinez, J. S. Andreu, J. Camacho and J. Faraudo, *Soft Matter*, 2012, **8**, 6039–6047.
81 R. Dreyfus, Q. Boehler, S. Lyttle, P. Gruber, J. Lussi, C. Chautems, S. Gervasoni, J. Berberat, D. Seibold, N. Ochsenbein-Kölble, M. Reinehr, M. Weisskopf, L. Remonda and B. J. Nelson, *Sci. Rob.*, 2024, **9**, eadh0298.
82 J. Yan, M. Bloom, S. C. Bae, E. Luijten and S. Granick, *Nature*, 2012, **491**, 578–581.
83 A. Ray and T. M. Fischer, *J. Phys. Chem. B*, 2012, **116**, 8233–8240.
84 L. Wittmann, M. Eigenfeld, K. Buchner, J. Meiler, H. Habisch, T. Madl, R. Kerpes, T. Becker, S. Berensmeier and S. P. Schwaminger, *Lab Chip*, 2024, **24**, 2987–2998.
85 J. Wu, W. Zou, Q. Lu, T. Zheng, Y. Li, T. Ying, Y. Li, Y. Zheng and L. Wang, *Adv. Sci.*, 2025, **12**, e2410351.
86 P. Zhang, H. Bachman, A. Ozcelik and T. J. Huang, *Annu. Rev. Anal. Chem.*, 2020, **13**, 17–43.

87 Y. Q. Fu, J. K. Luo, N. T. Nguyen, A. J. Walton, A. J. Flewitt, X. T. Zu, Y. Li, G. McHale, A. Matthews, E. Iborra, H. Du and W. I. Milne, *Prog. Mater. Sci.*, 2017, **89**, 31–91.
88 I. Leibacher, P. Reichert and J. Dual, *Lab Chip*, 2015, **15**, 2896–2905.
89 L. Y. Yeo and J. R. Friend, *Annu. Rev. Fluid Mech.*, 2014, **46**, 379–406.
90 L. V. King, *Proc. R. Soc. London, Ser. A*, 1934, **147**, 212–240.
91 A. A. Doinikov, *J. Fluid Mech.*, 1994, **267**, 1–22.
92 D. Ahmed, A. Ozcelik, N. Bojanala, N. Nama, A. Upadhyay, Y. Chen, W. Hanna-Rose and T. J. Huang, *Nat. Commun.*, 2016, **7**, 11085.
93 C. E. Owens, C. W. Shields, D. F. Cruz, P. Charbonneau and G. P. Lopez, *Soft Matter*, 2016, **12**, 717–728.
94 A. Tahmasebipour, L. Friedrich, M. Begley, H. Bruus and C. Meinhart, *J. Acoust. Soc. Am.*, 2020, **148**, 359.
95 R. Zhong, X. Xu, G. Tutoni, M. Liu, K. Yang, K. Li, K. Jin, Y. Chen, J. D. H. Mai, M. L. Becker and T. J. Huang, *Nat. Commun.*, 2025, **16**, 4144.
96 H. Ahmed, G. Destgeer, J. Park, J. H. Jung and H. J. Sung, *Adv. Sci.*, 2018, **5**, 1700285.
97 J. C. Giddings, *Sep. Sci.*, 1966, **1**, 123–125.
98 S. K. Wiedmer and M. L. Riekkola, *J. Chromatogr. A*, 2023, **1712**, 464492.
99 K. Zhao, Y. Wei, J. Dong, P. Zhao, Y. Wang, X. Pan and J. Wang, *Environ. Pollut.*, 2022, **297**, 118773.
100 L. Pitkanen, *J. Chromatogr. A*, 2025, **1748**, 465862.
101 I. K. Ventouri, S. Loeber, G. W. Somsen, P. J. Schoenmakers and A. Astefanei, *Anal. Chim. Acta*, 2022, **1193**, 339396.
102 S. Giordani, V. Marassi, A. Placci, A. Zattoni, B. Roda and P. Reschiglian, *Molecules*, 2023, **28**, 6201.
103 E. Furlani and Y. Sahoo, *J. Phys. D: Appl. Phys.*, 2006, **39**, 1724.
104 A. Barani, P. Mosaddegh, S. Haghjooy Javanmard, S. Sepehrirahnama and A. Sanati-Nezhad, *Sci. Rep.*, 2021, **11**, 22048.
105 P. Zemánek, G. Volpe, A. Jonáš and O. Brzobohatý, *Adv. Opt. Photonics*, 2019, **11**, 577–678.
106 S. Marbach, H. Yoshida and L. Bocquet, *J. Fluid Mech.*, 2020, **892**, A6.
107 N. Pamme, *Lab Chip*, 2006, **6**, 24–38.
108 H. Bruus, *Theoretical Microfluidics*, Oxford University Press, 2007.
109 R. I. Litvinov, H. Shuman, J. S. Bennett and J. W. Weisel, *Proc. Natl. Acad. Sci. U. S. A.*, 2002, **99**, 7426–7431.
110 M. Settnes and H. Bruus, *Phys. Rev. E:Stat., Nonlinear, Soft Matter Phys.*, 2012, **85**, 016327.
111 P. Cheng, M. J. Barrett, P. M. Oliver, D. Cetin and D. Vezenov, *Lab Chip*, 2011, **11**, 4248–4259.
112 V. Varmazyari, H. Habibiyan, H. Ghafoorifard, M. Ebrahimi and S. Ghafouri-Fard, *Sci. Rep.*, 2022, **12**, 12100.
113 S. Khashan, A. A. Odhah, M. Taha, A. Alazzam and M. Al-Fandi, *Sci. Rep.*, 2024, **14**, 13293.
114 M. Bier, *Electrophoresis: theory, methods, and applications*, Elsevier, 2013.
115 D. H. Gray and J. K. Mitchell, *J. Soil Mech. Found. Div.*, 1967, **93**, 209–236.
116 B. J. Kirby, *Micro-and Nanoscale Fluid Mechanics: Transport in Microfluidic Devices*, Cambridge University Press, 2010.
117 J. H. Masliyah and S. Bhattacharjee, *Electrokinetic and Colloid Transport Phenomena*, John Wiley & Sons, 2006.
118 C. Thomas, X. Lu, A. Todd, Y. Raval, T. R. Tzeng, Y. Song, J. Wang, D. Li and X. Xuan, *Electrophoresis*, 2017, **38**, 320–326.
119 H. A. Pohl, *J. Appl. Phys.*, 1958, **29**, 1182–1188.
120 M. Gouy, *J. Phys. Theor. Appl.*, 1910, **9**, 457–468.
121 D. L. Chapman, *London, Edinburgh Dublin Philos. Mag. J. Sci.*, 1913, **25**, 475–481.
122 P. Debye and E. Hückel, *Phys. Z.*, 1923, **24**, 185–206.
123 A. D. Hollingsworth and C. A. Silebi, *Langmuir*, 1996, **12**, 613–623.
124 L. Bureau, G. Coupier and T. Salez, *Eur. Phys. J. E:Soft Matter Biol. Phys.*, 2023, **46**, 111.
125 T. G. M. van de Ven, P. Warszynski and S. S. Dukhin, *J. Colloid Interface Sci.*, 1993, **157**, 328–331.
126 P. S. Williams, M. H. Moon and J. C. Giddings, *Colloids Surf., A*, 1996, **113**, 215–228.
127 S. M. Tabatabaei, T. G. M. van de Ven and A. D. Rey, *J. Colloid Interface Sci.*, 2006, **301**, 291–301.
128 A. S. Khair, *Curr. Opin. Colloid Interface Sci.*, 2022, **59**, 101587.
129 M. Rouhi Youssefi and F. J. Diez, *Electrophoresis*, 2016, **37**, 692–698.
130 S. Tottori, K. Misiunas, U. F. Keyser and D. J. Bonthuis, *Phys. Rev. Lett.*, 2019, **123**, 014502.
131 N. A. Mishchuk and P. V. Takhistov, *Colloids Surf., A*, 1995, **95**, 119–131.
132 Y. Ben and H.-C. Chang, *J. Fluid Mech.*, 2002, **461**, 229–238.
133 N. A. Mishchuk and N. O. Barinova, *Colloid J.*, 2011, **73**, 88–96.
134 B. H. Lapizco-Encinas, *Annu. Rev. Anal. Chem.*, 2024, **17**, 243–264.
135 M. L. Sin, V. Gau, J. C. Liao, D. A. Haake and P. K. Wong, *J. Phys. Chem. C*, 2009, **113**, 6561–6565.
136 J. J. Juarez, P. P. Mathai, J. A. Liddle and M. A. Bevan, *Lab Chip*, 2012, **12**, 4063–4070.
137 M. B. Sano, A. D. Rojas, P. Gatenholm and R. V. Davalos, *Ann. Biomed. Eng.*, 2010, **38**, 2475–2484.
138 J. Qin, X. Sun, Y. Liu, T. Berthold, H. Harms and L. Y. Wick, *Environ. Sci. Technol.*, 2015, **49**, 5663–5671.
139 A. Webster, J. Greenman and S. J. Haswell, *J. Chem. Technol. Biotechnol.*, 2010, **86**, 10–17.
140 D. Li, *Electrokinetics in Microfluidics*, Elsevier, 2004.
141 H.-C. Chang and L. Y. Yeo, *Electrokinetically-Driven Microfluidics and Nanofluidics*, Cambridge University Press, 2010.
142 W. B. Zimmerman, *Chem. Eng. Sci.*, 2011, **66**, 1412–1425.
143 A. Ramos, *Electrokinetics and Electrohydrodynamics in Microsystems*, Springer Science & Business Media, 2011.
144 Y. Lu, J. Gao, D. D. Zhang, V. Gau, J. C. Liao and P. K. Wong, *Anal. Chem.*, 2013, **85**, 3971–3976.
145 D. Tripathi, R. Jhorar, A. Borode and O. A. Bég, *Eur. J. Mech. B: Fluids*, 2018, **72**, 391–402.

146 S. Jiang, C. Li, D. Wang, J. Du, H. Ma, A. Nathan and J. Yu, *Langmuir*, 2025, **41**, 8312–8321.
147 P. R. C. Gascoyne and J. Vykoukal, *Electrophoresis*, 2002, **23**, 1973–1983.
148 Y. Ai, S. W. Joo, Y. Jiang, X. Xuan and S. Qian, *Electrophoresis*, 2009, **30**, 2499–2506.
149 N. Lewpiriyawong, C. Yang and Y. C. Lam, *Microfluid. Nanofluid.*, 2012, **12**, 723–733.
150 P. Cherukat and J. B. McLaughlin, *J. Fluid Mech.*, 2006, **263**, 1–18.
151 E. S. Asmolov, A. L. Dubov, T. V. Nizkaya, J. Harting and O. I. Vinogradova, *J. Fluid Mech.*, 2018, **840**, 613–630.
152 J. Su, X. Zheng and G. Hu, *Phys. Fluids*, 2023, **35**, 092010.
153 R. G. Cox and H. Brenner, *Chem. Eng. Sci.*, 1968, **23**, 147–173.
154 J.-P. Matas, J. F. Morris and É. Guazzelli, *J. Fluid Mech.*, 2004, **515**, 171–195.
155 J.-P. Matas, V. Glezer, É. Guazzelli and J. F. Morris, *Phys. Fluids*, 2004, **16**, 4192–4195.
156 Z. Zhang, V. Bertin, M. Arshad, E. Raphael, T. Salez and A. Maali, *Phys. Rev. Lett.*, 2020, **124**, 054502.
157 E. Yariv, *Phys. Fluids*, 2006, **18**, 031702.
158 L. Liang, Y. Ai, J. Zhu, S. Qian and X. Xuan, *J. Colloid Interface Sci.*, 2010, **347**, 142–146.
159 X. Lu, J. P. Hsu and X. Xuan, *Langmuir*, 2015, **31**, 620–627.
160 Q. Liang, C. Zhao and C. Yang, *Electrophoresis*, 2015, **36**, 731–736.
161 E. Yariv, *Soft Matter*, 2016, **12**, 6277–6284.
162 E. Alidoosti and H. Zhao, *Langmuir*, 2018, **34**, 5592–5599.
163 N. Cevheri and M. Yoda, *Lab Chip*, 2014, **14**, 1391–1394.
164 M. Rossi, A. Marin, N. Cevheri, C. J. Kähler and M. Yoda, *Microfluid. Nanofluid.*, 2019, **23**, 67.
165 B. M. Alexander and D. C. Prieve, *Langmuir*, 1987, **3**, 788–795.
166 J. J. Sousa, A. M. Afonso, F. T. Pinho and M. A. Alves, *Microfluid. Nanofluid.*, 2010, **10**, 107–122.
167 A. S. Khair and J. K. Kabarowski, *Phys. Rev. Fluids*, 2020, **5**, 033702.
168 A. Choudhary, T. Renganathan and S. Pushpavanam, *J. Fluid Mech.*, 2019, **874**, 856–890.
169 A. J. Hogg, *J. Fluid Mech.*, 2006, **272**, 285–318.
170 N. Cevheri and M. Yoda, *J. Nanotechnol. Eng. Med.*, 2014, **5**, 031009.
171 A. S. Khair and B. Balu, *Electrophoresis*, 2019, **40**, 2407–2414.
172 E. M. Purcell, *Am. J. Phys.*, 1977, **45**, 3–11.
173 A. Yee and M. Yoda, *Microfluid. Nanofluid.*, 2018, **22**, 113.
174 R. C. Jeffrey and J. R. A. Pearson, *J. Fluid Mech.*, 1965, **22**, 721–735.
175 D. Li and X. Xuan, *Phys. Fluids*, 2023, **35**, 092013.
176 D. Li and X. Xuan, *Phys. Rev. Fluids*, 2018, **3**, 074202.
177 M. Serhatlioglu, Z. Isiksacan, M. Ozkan, D. Tuncel and C. Elbuken, *Anal. Chem.*, 2020, **92**, 6932–6940.
178 G. Vishwanathan and G. Juarez, *Biomicrofluidics*, 2023, **17**, 064105.
179 R. Borthakur and U. Ghosh, *Phys. Rev. Fluids*, 2024, **9**, 023302.
180 R. Borthakur and U. Ghosh, *J. Fluid Mech.*, 2023, **954**, A48.
181 A. Lomeli-Martin, O. D. Ernst, B. Cardenas-Benitez, R. Cobos, A. S. Khair and B. H. Lapizco-Encinas, *Anal. Chem.*, 2023, **95**, 6740–6747.
182 A. Rao, A. S. Iglesias and M. Grzelczak, *J. Am. Chem. Soc.*, 2024, **146**, 18236–18240.
183 G. Zanderigo, F. Afghah, B. M. Colosimo and R. Raman, *Device*, 2025, **3**, 100927.
184 N. Vogel, L. de Viguerie, U. Jonas, C. K. Weiss and K. Landfester, *Adv. Funct. Mater.*, 2011, **21**, 3064–3073.
185 W. Lee, H. Amini, H. A. Stone and D. Di Carlo, *Proc. Natl. Acad. Sci. U. S. A.*, 2010, **107**, 22413–22418.
186 J. Aizenberg, P. V. Braun and P. Wiltzius, *Phys. Rev. Lett.*, 2000, **84**, 2997.
187 Q. Guo, C. Arnoux and R. Palmer, *Langmuir*, 2001, **17**, 7150–7155.
188 Y. Mino, S. Watanabe and M. T. Miyahara, *ACS Appl. Mater. Interfaces*, 2012, **4**, 3184–3190.
189 S. Watanabe, K. Inukai, S. Mizuta and M. T. Miyahara, *Langmuir*, 2009, **25**, 7287–7295.
190 M. A. Boles, M. Engel and D. V. Talapin, *Chem. Rev.*, 2016, **116**, 11220–11289.
191 J. F. Galisteo-Lopez, M. Ibisate, R. Sapienza, L. S. Froufe-Perez, A. Blanco and C. Lopez, *Adv. Mater.*, 2011, **23**, 30–69.
192 H. Zheng and S. Ravaine, *Crystals*, 2016, **6**, 54.
193 J. N. Anker, W. P. Hall, O. Lyandres, N. C. Shah, J. Zhao and R. P. Van Duyne, *Nat. Mater.*, 2008, **7**, 442–453.
194 J. P. Camden, J. A. Dieringer, J. Zhao and R. P. Van Duyne, *Acc. Chem. Res.*, 2008, **41**, 1653–1661.
195 F. Li, D. P. Josephson and A. Stein, *Angew. Chem., Int. Ed.*, 2011, **50**, 360–388.
196 Z. Cai, Z. Li, S. Ravaine, M. He, Y. Song, Y. Yin, H. Zheng, J. Teng and A. Zhang, *Chem. Soc. Rev.*, 2021, **50**, 5898–5951.
197 C. W. t Shields, C. D. Reyes and G. P. Lopez, *Lab Chip*, 2015, **15**, 1230–1249.
198 T. V. Nizkaya, E. S. Asmolov, J. Harting and O. I. Vinogradova, *Phys. Rev. Fluids*, 2020, **5**, 014201.
199 W. Tang, S. Zhu, D. Jiang, L. Zhu, J. Yang and N. Xiang, *Lab Chip*, 2020, **20**, 3485–3502.
200 J. F. Brady, *J. Fluid Mech.*, 2010, **667**, 216–259.
201 J. J. Erpenbeck, *Phys. Rev. Lett.*, 1984, **52**, 1333–1335.
202 W. Xue and G. S. Grest, *Phys. Rev. Lett.*, 1990, **64**, 419–422.
203 T. Yamada and S. Nose, *Phys. Rev. A:At., Mol., Opt. Phys.*, 1990, **42**, 6282–6284.
204 T. N. Phung, J. F. Brady and G. Bossis, *J. Fluid Mech.*, 2006, **313**, 181–207.
205 F. H. Rajab, C. M. Liauw, P. S. Benson, L. Li and K. A. Whitehead, *Food Bioprod. Process.*, 2018, **109**, 29–40.
206 M. Frenkel, P. Arya, E. Bormashenko and S. Santer, *J. Colloid Interface Sci.*, 2021, **586**, 866–875.
207 V. Muraveva, N. Lomadze, Y. D. Gordievskaya, P. Ortner, C. Beta and S. Santer, *Sci. Rep.*, 2024, **14**, 18342.
208 X. Zhao, Z. Chen, Y. Qiu and N. Hao, *Mater. Adv.*, 2023, **4**, 988–994.
209 M. Akella and J. J. Juarez, *ACS Omega*, 2018, **3**, 1425–1436.

210 Y. Gao, K. Liu, R. Lakerveld and X. Ding, *Nano Lett.*, 2022, **22**, 6907–6915.
211 S. Shabaniverki and J. J. Juarez, *Micromachines*, 2021, **12**, 935.
212 H. Sazan, S. Piperno, M. Layani, S. Magdassi and H. Shpaisman, *J. Colloid Interface Sci.*, 2019, **536**, 701–709.
213 Z. Chen, Z. Pei, X. Zhao, J. Zhang, J. Wei and N. Hao, *Chem. Eng. J.*, 2022, **433**, 133258.
214 L. Schmid, D. A. Weitz and T. Franke, *Lab Chip*, 2014, **14**, 3710–3718.
215 W. L. Ung, K. Mutafopulos, P. Spink, R. W. Rambach, T. Franke and D. A. Weitz, *Lab Chip*, 2017, **17**, 4059–4069.
216 L. Ren, Y. Chen, P. Li, Z. Mao, P. H. Huang, J. Rufo, F. Guo, L. Wang, J. P. McCoy, S. J. Levine and T. J. Huang, *Lab Chip*, 2015, **15**, 3870–3879.
217 S.-R. Yeh, M. Seul and B. I. Shraiman, *Nature*, 1997, **386**, 57–59.
218 L. Chen and A. T. Conlisk, *Biomed. Microdevices*, 2009, **11**, 251–258.
219 A. Bricard, J. B. Caussin, D. Das, C. Savoie, V. Chikkadi, K. Shitara, O. Chepizhko, F. Peruani, D. Saintillan and D. Bartolo, *Nat. Commun.*, 2015, **6**, 7470.
220 Z. Sheng, M. Zhang, J. Liu, P. Malgaretti, J. Li, S. Wang, W. Lv, R. Zhang, Y. Fan, Y. Zhang, X. Chen and X. Hou, *Natl. Sci. Rev.*, 2021, **8**, nwaa301.
221 Z. Chai, A. Childress and A. A. Busnaina, *ACS Nano*, 2022, **16**, 17641–17686.
222 A. P. Hsiao and M. J. Heller, *BioMed Res. Int.*, 2012, **2012**, 178487.
223 M. Mastrangeli, S. Abbasi, C. Varel, C. Van Hoof, J. P. Celis and K. F. Bohringer, *J. Micromech. Microeng.*, 2009, **19**, 83001.
224 K. D. Barbee, A. P. Hsiao, M. J. Heller and X. Huang, *Lab Chip*, 2009, **9**, 3268–3274.
225 K. K. Rangharajan and S. Prakash, *Analyst*, 2022, **147**, 3817–3821.
226 Y. H. Deng, E. Kheradmand, C. Pang, A. B. Siddik, J. Bai, I. Lieberman, P. Geiregat, D. Van Thourhout and Z. Hens, *ACS Appl. Mater. Interfaces*, 2025, **17**, 14243–14249.
227 J. Lv, H. Zhou, X. Ma, F. Liu, L.-M. Peng and C. Qiu, *ACS Nano*, 2025, **19**, 8997–9005.
228 T. Zhao, Y. Tan, Y. Li and X. Wang, *J. Colloid Interface Sci.*, 2025, **677**, 739–749.
229 Y. Park, J. Kim, M. Jeong, D. Shin, J. Jung, H. Kim, H. Jeong, H. Kim, Y.-H. Kim and S. Jeong, *Adv. Energy Mater.*, 2025, **15**, 2404141.
230 N. Göth and J. Dzubiella, *Commun. Phys.*, 2025, **8**, 65.
231 C.-M. Huang, A. Kucinic, J. A. Johnson, H.-J. Su and C. E. Castro, *Nat. Mater.*, 2021, **20**, 1264–1271.
232 M. J. Neuhoff, Y. Wang, N. J. Vantangoli, M. G. Poirier, C. E. Castro and W. G. Pfeifer, *Nano Lett.*, 2024, **24**, 12080–12087.
233 Z. Wang, Y. Mu, D. Lyu, M. Wu, J. Li, Z. Wang and Y. Wang, *Curr. Opin. Colloid Interface Sci.*, 2022, **61**, 101608.
234 C. Trugenberger, M. C. Diamantini, N. Poccia, F. S. Nogueira and V. M. Vinokur, *Quantum Rep.*, 2020, **2**, 388–399.
235 H.-Y. Xie, M. G. Vavilov and A. Levchenko, *Phys. Rev. B*, 2017, **96**, 161406.
236 C. Beneduce, F. Sciortino, P. Sulc and J. Russo, *ACS Nano*, 2023, **17**, 24841–24853.
237 R. Zhang, X. Zuo and F. Yin, *Chem Bio Eng.*, 2024, **2**, 71–86.
238 A. Kumar and V. Kumar, *J. Phys. Chem. C*, 2008, **112**, 3633–3640.
239 H. Dehne, A. Reitenbach and A. R. Bausch, *Sci. Rep.*, 2019, **9**, 7350.
240 P. Routh, R. K. Layek and A. K. Nandi, *Carbon*, 2012, **50**, 3422–3434.
241 J. J. Li, D. L. Kaplan and H. Zreiqat, *J. Mater. Chem. B*, 2014, **2**, 7272–7306.
242 A. De Pieri, Y. Rochev and D. I. Zeugolis, *npj Regener. Med.*, 2021, **6**, 18.
243 N. K. Rajendran, S. S. D. Kumar, N. N. Houreld and H. Abrahamse, *J. Drug Delivery Sci. Technol.*, 2018, **44**, 421–430.
244 F. Paladini and M. Pollini, *Materials*, 2019, **12**, 2540.
245 P. T.-L. Choi, G. Yip, L. G. Quinonez and D. J. Cook, *Crit. Care Med.*, 1999, **27**, 200–210.
246 J. Kreuter, *Colloidal Drug Delivery Systems*, CRC Press, 2014.
247 U. Lohmann, F. Lüönd and F. Mahrt, *An Introduction to Clouds: From the Microscale to Climate*, Cambridge University Press, 2016.
248 C.-W. Chen, C.-T. Hou, C.-C. Li, H.-C. Jau, C.-T. Wang, C.-L. Hong, D.-Y. Guo, C.-Y. Wang, S.-P. Chiang, T. J. Bunning, I.-C. Khoo and T.-H. Lin, *Nat. Commun.*, 2017, **8**, 727.
249 S. A. Asher, J. M. Weissman, A. Tikhonov, R. D. Coalson and R. Kesavamoorthy, *Phys. Rev. E:Stat., Nonlinear, Soft Matter Phys.*, 2004, **69**, 066619.
250 J. W. Haus, H. S. Zhou, S. Takami, M. Hirasawa, I. Honma and H. Komiyama, *J. Appl. Phys.*, 1993, **73**, 1043–1048.
251 X. Lu, M. Rycenga, S. E. Skrabalak, B. Wiley and Y. Xia, *Annu. Rev. Phys. Chem.*, 2009, **60**, 167–192.
252 N. G. Khlebtsov and L. A. Dykman, *J. Quant. Spectrosc. Radiat. Transfer*, 2010, **111**, 1–35.
253 L. Lin, X. Peng, M. Wang, L. Scarabelli, Z. Mao, L. M. Liz-Marzan, M. F. Becker and Y. Zheng, *ACS Nano*, 2016, **10**, 9659–9668.
254 D. Kim, J. Resasco, Y. Yu, A. M. Asiri and P. Yang, *Nat. Commun.*, 2014, **5**, 4948.
255 S. Yoo and Q. H. Park, *Nanophotonics*, 2019, **8**, 249–261.
256 A. J. Willis, S. P. Pernal, Z. A. Gaertner, S. S. Lakka, M. E. Sabo, F. M. Creighton and H. H. Engelhard, *Int. J. Nanomed.*, 2020, **15**, 4105–4123.
257 S. J. Ebbens, *Curr. Opin. Colloid Interface Sci.*, 2016, **21**, 14–23.
258 A. A. Harraq, B. D. Choudhury and B. Bharti, *Langmuir*, 2022, **38**, 3001–3016.
259 Y. He, J. Liu, X. Yang, J. Yang and F. Jiao, *Mater. Today Bio*, 2025, **33**, 102072.
260 Z. Yi, D. Cui, J. Tang, X. Ma and W. Wang, *Chem. Commun.*, 2025, **61**, 14649–14652.
261 D. Li, H. Wei, H. Fang and Y. Gao, *Photonics*, 2024, **11**, 421.

262 Z. Peng and R. Kapral, *Soft Matter*, 2024, **20**, 1100–1113.
263 J. Ge, L. He, Y. Hu and Y. Yin, *Nanoscale*, 2011, **3**, 177–183.
264 O. D. Velev and K. H. Bhatt, *Soft Matter*, 2006, **2**, 738–750.
265 F. Candelier, R. Mehaddi, B. Mehlig and J. Magnaudet, *J. Fluid Mech.*, 2023, **954**, A25.
266 X. Zhang, J. Minten and B. Rallabandi, *Phys. Rev. Fluids*, 2024, **9**, 044303.
267 M. Baalousha, J. Lead, Y. Ju-Nam and P. Wilderer, *Treatise Water Sci.*, 2011, **3**, 89–129.
268 Y. Shi and T. L. Beck, *J. Chem. Phys.*, 2013, **139**, 044504.
269 A. Kostopoulou and A. Lappas, *Nanotechnol. Rev.*, 2015, **4**, 595–624.
270 R. W. Ditchburn, *Light*, Courier Corporation, 2013.
271 N. Bélicard, M. J. Niémet-Mabiala, J.-N. Tourvieille and P. Lidon, *Rheol. Acta*, 2023, **62**, 71–89.